

1 **Using results from the PliomIP ensemble to investigate the Greenland Ice Sheet during**
2 **the mid-Pliocene warm period**

3 by

4 **A. M. Dolan**¹, S. J. Hunter¹, D. J. Hill^{1,2}, A. M. Haywood¹, S. J. Koenig³, B. L. Otto-
5 Bliesner⁴, A. Abe-Ouchi^{5,6}, F. Bragg⁷, W.-L. Chan⁵, M. A. Chandler⁸, C. Contoux⁹, A. Jost¹⁰,
6 Y. Kamae¹¹, G. Lohmann¹², D. J. Lunt⁷, G. Ramstein¹³, N. A. Rosenbloom⁴, L. Sohl¹⁴, C.
7 Stepanek¹², H. Ueda¹¹, Q. Yan¹⁵, and Z. Zhang^{15,16}

- 8 1. School of Earth and Environment, Earth and Environment Building, University of
9 Leeds, Leeds, LS2 9JT, UK
10 2. British Geological Survey, Keyworth, Nottingham, UK
11 3. Department of Geosciences, University of Massachusetts, 611 N. Pleasant St,
12 Amherst, MA 01003, USA
13 4. National Center for Atmospheric Research, Boulder, Colorado, USA
14 5. Atmosphere and Ocean Research Institute, University of Tokyo, Kashiwa, Japan
15 6. Research Institute for Global Change, JAMSTEC, Yokohama, Japan
16 7. School of Geographical Sciences, University of Bristol, University Road, Bristol, BS8
17 1SS, UK
18 8. Columbia University – NASA/GISS, New York, NY, USA
19 9. Aix-Marseille Université, CNRS, IRD, CEREGE UM34, 13545 Aix en Provence,
20 France.
21 10. Sorbonne Universités, UPMC Univ Paris 06, UMR 7619, Metis, F-75005, Paris, France
22 11. Graduate School of Life and Environmental Sciences, University of Tsukuba,
23 Tsukuba, Japan
24 12. Alfred Wegener Institute, Helmholtz Centre for Polar and Marine Research
25 13. Laboratoire des Sciences du Climat et de l'Environnement, Saclay, France
26 14. Columbia University – NASA/GISS, New York, NY, USA
27 15. Bjerknes Centre for Climate Research, Uni Research Climate, Bergen,
28 Norway
29 16. Institute of Atmospheric Physics, Chinese Academy of Sciences, Beijing, China

30
31 Email correspondence to Aisling M. Dolan (a.m.dolan@leeds.ac.uk)

32

33

34

35

36 **Abstract**

37 During the mid-Pliocene Warm Period (3.264 to 3.025 million years ago), global mean temperature
38 was similar to that predicted for the end of this century, and atmospheric carbon dioxide
39 concentrations were higher than pre-industrial levels. Sea level was also higher than today, implying
40 a significant reduction in the extent of the ice sheets. Thus, the mid-Pliocene Warm Period provides a
41 natural laboratory in which to investigate the long-term response of the Earth's ice sheets and sea level
42 in a warmer-than-present-day world.

43 At present, our understanding of the Greenland ice sheet during the warmest intervals of the mid-
44 Pliocene is generally based upon predictions using single climate and ice sheet models. Therefore, it is
45 essential that the model dependency of these results is assessed. The Pliocene Model Intercomparison
46 Project (PlioMIP) has brought together nine international modelling groups to simulate the warm
47 climate of the Pliocene. Here we use the climatological fields derived from the results of the 15
48 PlioMIP climate models to force an offline ice sheet model.

49 We show that Pliocene ice sheet reconstructions are highly dependent upon the forcing climatology
50 used, with Greenland reconstructions ranging from an ice-free state to a near modern ice sheet. An
51 analysis of the surface albedo variability between the climate models over Greenland offers insights
52 into the drivers of inter-model differences. As we demonstrate that the climate model dependency of
53 our results is high, we highlight the necessity of data-based constraints of ice extent in developing our
54 understanding of the Pliocene Greenland ice sheet.

55 **1. Introduction**

56 The response of the Earth's ice sheets to a warming climate is a critical uncertainty in future
57 predictions of climate and sea level (Church et al., 2013; Masson-Delmotte et al., 2013; Vaughan et
58 al., 2013). Therefore, there is increasing interest in understanding the nature and behaviour of the
59 major ice sheets during warm intervals in Earth history. The Pliocene Epoch, and more specifically
60 warm 'interglacial' events within the mid-Pliocene, is a particularly well documented pre-Quaternary
61 environment which has become the focus for intense study within the Pliocene Model
62 Intercomparison Project (PlioMIP; Haywood et al., 2010; 2011a). The mid-Pliocene warm period
63 (mPWP; 3.26 to 3.025 million years ago; Dowsett et al., 2010) is predicted to have been between 2°C
64 and 3°C warmer than pre-industrial (Haywood et al., 2009; 2013; Lunt et al., 2010) and estimates of
65 atmospheric carbon dioxide (CO₂) concentrations suggest levels of up to 450 *ppmv* (Pagani et al.,
66 2010; Seki et al., 2010). Although in recent literature the terms mid-Piacenzian or Late Pliocene
67 warm events have been used, here we retain consistency with the original PlioMIP naming convention

68 and use the mPWP. The IPCC 5th Assessment Report states with high confidence that global mean
69 sea level was above present (up to 20 m) during warm intervals of the mid-Pliocene (Masson-
70 Delmotte et al., 2013) and individual records of sea level high-stands (~20 m) support the reduction in
71 the extent of the ice sheets at this time (e.g. Miller et al., 2012; Rovere et al., 2014; Rohling et al.,
72 2014).

73 Proxy records of palaeotemperature derived from ice cores (Dahl-Jensen et al., 1998; Cuffey and
74 Marshall, 2000; Johnsen et al., 2001; Rasmussen et al., 2006) and numerical modelling (Otto-Bliesner
75 et al., 2006; Overpeck et al., 2006; van de Berg et al., 2011; Born et al., 2012; Quiquet et al., 2013;
76 Stone et al., 2013) of more recent interglacials demonstrate that the Greenland ice sheet (GrIS) has a
77 large sensitivity to high-latitude warming. However, there is little proximal evidence to indicate the
78 volume or extent of the GrIS during the warmest intervals of the mid-Pliocene. Evidence of long
79 lasting subaerial soil formation at the base of the central Greenland Ice Sheet have been suggested as
80 evidence for persistent reduction in Pliocene ice, but the soils have not been positively dated as
81 relating to this period (Bierman et al., 2014). The presence of forest fragments in the Kap København
82 Formation in the far North of Greenland up until 2.4 Ma (Funder et al., 2001) suggests that this area
83 may have been ice-free through intervals of the mid-Pliocene. Fragments of evergreen taiga forest in
84 Pliocene sediments at Ile de France (Bennike et al., 2002) also suggest that ice marginal regions were
85 much warmer during the Pliocene. Records from the central Labrador Sea suggest that landmasses
86 adjacent to Greenland, such as Ellesmere and Baffin Island, show a predominance of evergreen forest
87 during intervals of the Pliocene (De Vernal and Mudie, 1989; Thompson and Flemming, 1996;
88 Ballantyne et al., 2006; Csank et al., 2011). Additionally, temperature estimates from peat deposits in
89 the Canadian High Arctic (Beaver Pond) suggest elevated Pliocene Arctic temperatures (Ballantyne et
90 al., 2010). Although there are no Pliocene temperature records from Greenland against which to test
91 the climate model simulations, there is generally a cool bias in the models compared to the available
92 data in the Northern high latitudes (Dowsett et al., 2012; Salzmann et al., 2013).

93 While useful, proxy evidence is too sparse and uncertain to enable a detailed reconstruction of the
94 extent and location of mid-Pliocene ice sheets. Therefore, a variety of modelling frameworks have
95 been adopted in order to simulate the mass balance of the GrIS and reconstruct potential ice sheet
96 configurations during the mid-Pliocene (Lunt et al., 2008; 2009; Hill, 2009; Hill et al., 2010; Dolan et
97 al., 2011; Koenig et al., 2011; 2014a; 2014b). These modelling frameworks have generally included
98 the offline coupling of an ice sheet model (ISM) to a climate model, and have been limited to the use
99 of three climate models; the UKMO UM (UK Met Office Unified Model; e.g. Hill et al., 2010; Dolan
100 et al., 2011), GENESIS (e.g. Koenig et al., 2011) and multiple versions of CAM (Community
101 Atmosphere Model; e.g. Yan et al., 2014). Although all available simulations suggest that the GrIS
102 was reduced in size during the mid-Pliocene warm period, the model dependency of the results is yet
103 to be robustly assessed. The extent to which ice sheet reconstructions are dependent on the ISM

104 employed is addressed through a sub-project of PlioMIP, entitled the Pliocene Ice Sheet Modelling
105 Intercomparison Project (PLISMIP; Dolan et al., 2012). Results from Koenig et al. (2014b) suggest
106 that ISM dependency is low. Here, we will address the question of climate model dependency
107 utilising climate model outputs from PlioMIP (Chan et al., 2011; Bragg et al., 2012; Contoux et al.,
108 2012; Stepanek and Lohmann, 2012; Yan et al., 2012; Kamae and Ueda, 2012; Zhang and Yan, 2012;
109 Zhang et al., 2012; Chandler et al. 2013; Rosenbloom et al., 2013) to force the British Antarctic
110 Survey ISM (BASISM). Results from PlioMIP present a unique opportunity to sample differences in
111 model predictions of climate and how this impacts on our reconstruction of the GrIS.

112 Initially a summary of the PlioMIP experimental design will be provided, followed by a description of
113 the offline coupling method adopted for the ISM simulations in this study, which will include details
114 of the climate differences over Greenland as derived from the PlioMIP ensemble. A discussion of the
115 differences between equilibrium-state ice sheet simulations using the climatological forcing from the
116 fifteen different climate model experiments in the PlioMIP ensemble will follow and we will conclude
117 with an assessment of the potential causes of any discrepancies and suggestions for future modelling
118 strategies of the mPWP GrIS.

119 The aims of this paper can be summarised as:

- 120 • To assess the extent to which GrIS reconstructions for the mPWP are dependent upon the
121 climate model used to force the ISM.
- 122 • To understand the potential reasons for any differences between the simulated GrISs by
123 considering factors which may affect the climate representation over Greenland in the
124 PlioMIP models.
- 125 • To inform decisions regarding the prescription of the GrIS in subsequent climate model
126 experiments (e.g. the second phase of PlioMIP).

127 **2. Methods**

128 **2.1 Climate Model Forcing (PlioMIP)**

129 **2.1.1 The PlioMIP ensemble**

130 In order to systematically examine uncertainties in numerical model predictions of the mPWP,
131 PlioMIP (Haywood et al., 2010; 2011a) was initiated as a component of PMIP (Palaeoclimate Model
132 Intercomparison Project). PMIP's aim is to provide a means for co-ordinating palaeoclimate
133 modelling and model-evaluation activities in order to understand the mechanisms of climate change

134 and the role of climate feedbacks under past climate conditions (Braconnot et al., 2012). Previous
135 comparisons of Pliocene simulations had been limited to at most three different climate models and
136 had incorporated different approaches to implementing the Pliocene boundary conditions (e.g.
137 Haywood et al., 2000; 2009).

138 PlioMIP established the design for two initial experiments. Experiment 1 used atmosphere-only
139 climate models (AGCMs) and is detailed fully in Haywood et al. (2010). Experiment 2 utilised
140 coupled atmosphere-ocean climate models (AOGCMs) and is described in Haywood et al. (2011a).
141 Here the atmospheric and topographic fields from both the AGCMs and the AOGCMs in PlioMIP
142 (Table 1) will be used to force an offline shallow ice approximation ISM (BASISM; see Section 2.2).

143 The boundary conditions applied to all climate models of PlioMIP are described specifically in
144 Haywood et al. (2010) and Haywood et al. (2011a) respectively. In brief, both experiments utilised
145 the US Geological Survey PRISM3 boundary condition data set (Dowsett et al., 2010). PRISM3 is an
146 improved dataset in terms of data coverage compared to its predecessor (PRISM2; Dowsett et al.,
147 1999) and includes information on monthly SSTs and sea ice distributions, vegetation cover, sea level,
148 ice sheet extent and topography. Vegetation cover is based on the palaeobotanical reconstruction of
149 Salzmänn et al. (2008) and topography is derived from the Sohl et al (2009) palaeogeographic
150 reconstruction. The PRISM3 ice sheets applied in the climate models were derived from offline ISM
151 experiments forced with climatological fields from the Hadley Centre Atmosphere-only climate
152 model (Fig. 1; HadAM3; Hill, 2009), and represent an ice sheet that is consistent with the rest of the
153 PRISM3 reconstruction. For the AGCMs the SST and sea ice distribution was fixed according to
154 PRISM3, whereas the AOGCMs predicted their own Pliocene sea surface conditions.

155 In all of the PlioMIP experiments, the atmospheric concentration of CO₂ was set to 405 *ppmv*
156 (Haywood et al., 2010; 2011a). This is slightly higher than the previous standard PRISM2 level (400
157 *ppmv*), but still falls well within the uncertainty limits of current CO₂ proxy records (e.g. Pagani et al.,
158 2010; Seki et al., 2010; Bartoli et al., 2011). All other trace gases were specified at a pre-industrial
159 concentration and the selected orbital configuration was unchanged from modern (Haywood et al.,
160 2010).

161 Each of the PlioMIP models were set-up with PRISM3 boundary conditions as described above and
162 then run for a minimum integration length of 50 years for the AGCMs and 500 years for the
163 AOGCMs. Average climatological forcing fields were derived from the final 30 years of the
164 simulation. Each modelling group's standard pre-industrial simulation was used as a control run.

165 Details of participating groups and climate models can be found in Table 1. Simulations from seven
166 AGCMs and eight AOGCMs were completed and results submitted to PlioMIP. The AGCMs and

167 AOGCMs sample differing levels of complexity and resolution, from higher-resolution IPCC AR5-
168 class models to intermediate resolution models (Haywood et al., 2013).

169 **2.1.2 Climatological Forcing over Greenland**

170 Greenland mean annual temperature and precipitation, and summer temperature anomalies between
171 the mid-Pliocene and the pre-industrial for each of the PlioMIP AGCMs and AOGCMs are shown in
172 Figures 2, 3 and 4. Over Greenland simulated mid-Pliocene climates from the AGCMs show an
173 increase in mean annual temperature of between 11.9°C and 14.1°C, whereas the range predicted
174 from the AOGCMs is much greater (5.3°C to 12.8°C; Table 3). For the AGCMs, mid-Pliocene mean
175 annual precipitation levels over the Greenland region (Table 3) increase compared to pre-industrial in
176 models. All AOGCMs show an increase in mid-Pliocene precipitation of between 0.2 mm day⁻¹ and
177 0.8 mm day⁻¹. Simulated mid-Pliocene summer temperatures were on average 12.6°C warmer over
178 Greenland for the AGCMs and 12.3°C warmer in the AOGCMs. However, the average for the
179 AOGCMs is lowered due to MRI-AOGCM simulating a warming of 4°C, whereas all other AOGCMs
180 fall between 11.6°C and 15°C of warming in the Pliocene relative to the pre-industrial control
181 simulation.

182

183 **2.2 Ice Sheet Modelling Framework**

184 In this study we used BASISM, which has previously been applied to study Pliocene ice sheets (Hill
185 et al., 2007; Hill, 2009; Hill et al., 2010; Dolan et al., 2011). BASISM is a finite difference,
186 thermomechanical, shallow ice approximation (SIA) ISM, utilising an unconditionally stable, implicit
187 numerical solution of the non-linear simultaneous equations of ice flow. BASISM is similar to other
188 SIA models described by Huybrechts (1990), Ritz et al. (2001) and Rutt et al. (2009) and a more
189 detailed discussion of the numerical formulations behind BASISM can be found in Hindmarsh (1993,
190 1996, 1999, 2001). As well as the internal glaciological dynamics, interactions with the bedrock are
191 simulated with a simple model of elastic rebound, with a rebound timescale of 3000 years (Le Meur
192 and Huybrechts, 1996). The bedrock height for all initial conditions is recalculated using this model,
193 on the assumption of isostatic equilibrium and then the bedrock is allowed to dynamically evolve and
194 adjust during subsequent ice sheet changes.

195 For this study, BASISM was run on a 20 km × 20 km grid, with 21 vertical layers, in a domain
196 covering the modern grounded GrIS. The ISM is forced using climatological fields of mean annual
197 temperature (Fig. 2) and precipitation (Fig. 3) and warmest mean monthly temperature (July; Fig.4)

198 from each of the PlioMIP ensemble members following the method of Hill (2009). An exponential
199 function is used to convert temperatures into the number of positive degree days (PDD; Reeh, 1991),
200 which shows a high level of correlation between warmest month temperatures and observations of
201 present day melt (Hill, 2009). Bilinear interpolation was used to downscale the meteorological fields
202 from the original climate model grid onto the higher resolution ISM grid. Downscaling is problematic
203 in that the coarse horizontal resolution of the climate model is inadequate to resolve the steep
204 topographic slopes around the edges of Greenland (Thompson and Pollard, 1997; Ridley et al., 2005).
205 This is partly addressed by applying a uniform and constant lapse rate correction to resolve for the
206 difference in climate model and ISM topography, both in the initial conditions and as the ice sheet
207 surface evolves during the simulation. The standard lapse rate used within BASISM is $-6.0^{\circ}\text{C km}^{-1}$,
208 which lies within modern observations of lapse rates on Greenland (Steffen and Box, 2001; Hanna et
209 al., 2005). Currently, there is no known similar simple relationship between precipitation and altitude.
210 Precipitation over the GrIS is highly non-linear, with synoptic patterns of atmospheric circulation
211 tending to drive patterns of accumulation (Schuenemann and Cassano, 2009). Combined model
212 simulations and tree-ring isotopes have shown that the dominant patterns of Pliocene North Atlantic
213 atmospheric circulation are likely to have remained similar to today (Hill et al., 2011). Although some
214 direct effects of altitude and temperature will occur as the ice sheet evolves, one of the key changes
215 will be feedbacks on atmospheric circulation, which can only be modelled in a coupled ice sheet–
216 climate model (Mayewski et al., 1994). Where downscaling methods do exist (e.g. Ritz et al., 1997),
217 the ratio of precipitation change with temperature change is poorly constrained (Charbit et al., 2002).
218 Therefore, no correction for precipitation has been made within the ice sheet modelling experiments
219 presented here.

220 The PDD method was employed to convert the climate fields into a melt rate (Reeh, 1991;
221 Braithwaite, 1995), and is well established in coupled atmosphere-ice sheet palaeoclimate modelling
222 studies (e.g. DeConto and Pollard, 2003; Lunt et al., 2008a; 2008b; 2009). The PDD technique
223 assumes that the melting of the ice sheet surface can be fully described by three physical constants
224 (melt rate or PDD factor of ice and snow and the maximum fractional refreezing rate (W_{max})) and the
225 temperature record. Although many other factors could contribute this method has been shown to
226 have some physical justification (Ohmura, 2001). Standard PDD parameters for ice (α_i) and snow
227 (α_s) are set to $\alpha_i = 8 \text{ mm day}^{-1} \text{ }^{\circ}\text{C}^{-1}$ and $\alpha_s = 3 \text{ mm day}^{-1} \text{ }^{\circ}\text{C}^{-1}$ respectively, which is within
228 observations of different modern day climates (Braithwaite, 1995). Further developments of the PDD
229 method have been used in previous studies, but they rely on additional glaciological parameters that
230 may not remain constant in palaeoclimate scenarios, thus it is unclear how to assign them for the
231 Pliocene (Janssens and Huybrechts, 2000; Tarasov and Peltier, 2002)

232 The aforementioned “standard” glaciological parameters (i.e. lapse rate, and the PDD factors of ice
233 and snow) used in BASISM were originally tuned for a HadAM3 experiment (Hill, 2009), so that the
234 best representation of the modern GrIS and East Antarctic Ice Sheet (EAIS) were simulated.
235 However, these parameter values are still poorly constrained, resulting in highly variable ice sheet
236 volumes and extents depending on the exact values prescribed (Ritz et al., 1997; Lunt et al., 2008b;
237 Stone et al., 2010). Stone et al. (2010) demonstrated that the ice sheet extent is predominantly
238 dependent on the PDD factors and the lapse rate, and therefore we have chosen to vary these
239 parameters in order to obtain an additional estimate of uncertainty on our ISM-based GrIS
240 reconstructions.

241 The typical annual lapse rate used for a variety of studies on Greenland (e.g. Ridley et al., 2005;
242 Huybrechts and de Wolde, 1999; Vizcaíno et al., 2008) ranges from $-6.0^{\circ}\text{C km}^{-1}$ to $-8.0^{\circ}\text{C km}^{-1}$ and
243 therefore here we will test values within this range (Table 2). The PDD parameter values for ice and
244 snow vary much more within the literature and previous modelling studies. The standard value for ice
245 used by many modellers is $8 \text{ mm day}^{-1} \text{ }^{\circ}\text{C}^{-1}$ (e.g. Huybrechts and de Wolde, 1999; Ritz et al., 1997),
246 although Braithwaite (1995) suggested that the value could be as much as $20 \text{ mm day}^{-1} \text{ }^{\circ}\text{C}^{-1}$.
247 Modelling studies for the Pliocene Greenland (e.g. Lunt et al., 2008a) have tested a range of PDD
248 parameters from *low* PDD factors ($\alpha_i = 8 \text{ mm day}^{-1} \text{ }^{\circ}\text{C}^{-1}$ and $\alpha_s = 3 \text{ mm day}^{-1} \text{ }^{\circ}\text{C}^{-1}$; the same as
249 BASISM standard) to very high PDD factors ($\alpha_i = 64 \text{ mm day}^{-1} \text{ }^{\circ}\text{C}^{-1}$ and $\alpha_s = 24 \text{ mm day}^{-1} \text{ }^{\circ}\text{C}^{-1}$) and
250 have shown that the higher end of these ranges do not lead to a good simulation of the modern GrIS.
251 Here we vary PDD factors conservatively between $\alpha_s = 3 \text{ mm day}^{-1} \text{ }^{\circ}\text{C}^{-1}$ and $\alpha_s = 6 \text{ mm day}^{-1} \text{ }^{\circ}\text{C}^{-1}$ for
252 snow and $\alpha_i = 5 \text{ mm day}^{-1} \text{ }^{\circ}\text{C}^{-1}$ and $\alpha_i = 14 \text{ mm day}^{-1} \text{ }^{\circ}\text{C}^{-1}$ for ice (Table 2).

253 Although it is possible to use statistical methods such as Latin Hypercube Sampling (LHS) to define
254 random plausible parameter sets within a given range (e.g. Stone et al., 2010), here we simply choose
255 to co-vary parameters. Table 2 shows the parameter values tested here, which equals 48 parameter
256 permutations for each simulation based on the forcing from a specific climate model. In every ISM
257 simulation, absolute temperatures and precipitation values were used to force the ISM, and no
258 correction was made to account for temperature biases in each model’s simulation of the pre-
259 industrial (*cf.* Lunt et al., 2009). BASISM was run for 50 000 years, which is enough time for the
260 simulated ice sheet to come into geometric and thermal equilibrium with the forcing climate.

261 Prior to simulating the Pliocene GrIS, control cases were run in order to enable an assessment of the
262 modelling framework for the pre-industrial. For the pre-industrial simulations, BASISM was
263 initialised from a modern ice configuration. Initially it is useful to determine whether the pre-
264 industrial control climate from each model produces a sensible reconstruction of the present
265 Greenland ice sheet using BASISM with the range of glaciological parameters that are identified in
266 Table 2. In order to analyse the ice sheet geometries from the 48 experiments undertaken for each of

267 the PlioMIP climate models, we have chosen two performance metrics to investigate for each model
268 simulation. Following the methods of Stone et al. (2010), the difference in total ice volume compared
269 to estimated modern volume will be used as an overall diagnostic of how well each simulation
270 reconstructs the observations of ice thickness. The second performance metric will be the Root Mean
271 Square Error (RMSE), which is a measure of the spatial fit of the ice sheet thickness reconstruction
272 over the Greenland domain. The RMSE describes the magnitude of the differences between two
273 fields (e.g. observed ice thickness and simulated ice thickness). In both cases, lower values describe a
274 better match between the modelled and the observed GrIS. We use the digital elevation model (DEM)
275 of Bamber et al. (2001), interpolated on to the ISM grid (20 km resolution), to calculate observed ice
276 sheet volume and thickness. This technique will also allow the definition of optimal parameter sets
277 (within the envelope of parameter values tested) which gives each forcing climate model the “best”
278 estimate of the present GrIS. These parameter sets were then used with each of the climate forcings
279 from the PlioMIP ensemble.

280 **3. Results**

281 **3.1 Greenland Ice Sheet Simulations**

282 **3.1.1 Pre-Industrial Control Greenland Ice Sheets**

283 For the pre-industrial control experiments, BASISM was initialised from the modern GrIS. Figures
284 5a (AGCMs) and 5b (AOGCMs) summarise the sensitivity of modelled GrIS volume to the three
285 tuneable glaciological parameters (Table 2). For most of the PlioMIP climate model inputs, the
286 choice of parameter values for atmospheric lapse rate and the PDD factors of ice and snow have little
287 impact on the resulting GrIS volume (with the exception of HadAM3 and the fully coupled version of
288 MIROC, where the final volume depends on the choice of the parameter set; Fig. 5b). This is due to
289 the modern ablation zone being constrained to the steep slopes on the periphery of the ice sheet and
290 the constraints applied at the ice sheet grounding line. The parameter set for each PlioMIP model that
291 gives the optimal ice sheet in terms of total ice volume or RMSE of ice thickness for steady-state
292 conditions in comparison to modern observations, is also shown in Figures 5a and 5b. Based on the
293 diagnostics chosen here, the optimal parameter sets are never equal to the standard parameter values
294 used within BASISM, although the impact of this on the pre-industrial GrIS is minimal.

295 For ease of comparison, if we consider using the standard BASISM parameters, all forcing
296 climatologies produce a GrIS which is similar to modern observations. However, the ISM
297 consistently overestimates ice volume by between +3% and +17%. Comparing the spatial differences

298 between Bamber et al. (2001) and the PlioMIP-based ISM simulations, there are similar biases in
299 elevation (Fig. 6) between the different climate forcings. Over central Greenland, some BASISM
300 simulations produce ice sheets that are too low (~200 to 400 m) in comparison to observations (Fig. 6)
301 although others (notably CAM3.1, COSMOS (AGCM and AOGCM), NorESM (AGCM and
302 AOGCM)) are very close to observations in these regions. Consistent with other ISMs (e.g. Koenig et
303 al, 2014b), all BASISM simulations produce ice sheets that are too high (up to ~800 m) at the ice
304 sheet margins (Fig. 6). These largest deviations from observations occur in the regions of fast ice
305 sheet flow around the ice sheet margins. At these locations there are inherent problems with both the
306 relatively coarse resolution climate model and the ISM when simulating areas of steep topography
307 and complex dynamics. Additionally, as a large proportion (~40%) of the ice loss in Greenland
308 occurs through iceberg calving (Huybrechts et al., 1991) and such grounding line physics are omitted
309 from this SIA ISM, it is expected that ice loss at the margin would be underestimated (Fig. 6). For
310 smaller simulated ice sheets where ice terminates on land (such as those in the Pliocene e.g. PRISM3;
311 Fig. 1), problems associated with ice dynamics such as calving are anticipated to have less of an
312 influence on the reconstruction.

313 The ranking between the simulations depends upon the choice of metric (volumetric or spatial) and
314 thus no one climatological forcing stands out as giving the best representation of the present GrIS.
315 Therefore these metrics will be considered separately in the analysis of Pliocene results. RMSE
316 values for each PlioMIP model based on the optimal parameter sets range from 250 to 305 m, and
317 there is no discernible difference in skill at reproducing the modern GrIS between the AGCMs (Fig.
318 5a) and the AOGCMs (Fig. 5b). Considering both the AGCMs and AOGCMs, the parameter set for
319 each model which gives the smallest RMSE, simulates a difference in volume between the models of
320 $3.01 \times 10^6 \text{ km}^3$ and $3.47 \times 10^6 \text{ km}^3$. Using the standard parameter set used in BASISM, the volume
321 difference for the pre-industrial is similar ($3.02 \times 10^6 \text{ km}^3$ and $3.44 \times 10^6 \text{ km}^3$). In summary, none of
322 the simulated ice sheets show any significant biases beyond those inherent when using a SIA ISM
323 (see also Ritz et al. 1997; Saito and Abe-Ouchi, 2005). This provides confidence in the results of the
324 Pliocene ISM simulations using the same modelling framework.

325 **3.1.2 Pliocene Greenland Ice Sheets**

326 For the mid-Pliocene runs, BASISM was initialised from the PRISM3 ice configuration (Dowsett et
327 al., 2010; Fig. 1), consistent with the climate model forcing. Figure 7 shows the simulated GrIS
328 volume for each of the PlioMIP ensemble members using the different glaciological parameters listed
329 in Table 2. In contrast to the pre-industrial ice sheets, Pliocene simulations are much more sensitive
330 to the chosen parameter values within the ISM. This is consistent with results presented by Robinson
331 et al. (2011) using a different modelling framework, which show that the modern GrIS is less

332 sensitive to changes in melt parameters than ice sheet reconstructions for the warmer-than-modern
333 Eemian Interglacial (ca. 130-115 ka BP). In all cases, the use of the standard, the volumetrically
334 optimal or the spatially optimal parameters within BASISM has a significant impact on the resulting
335 Pliocene GrIS reconstruction (Fig. 7).

336 Figure 8 shows the surface mass balance (SMB) calculated by BASISM for the PlioMIP climatologies
337 from the initial ISM time-step. BASISM simulates a positive SMB over the PRISM3 ice sheet region
338 for the majority of PlioMIP climate forcings and over the southern and western parts of Greenland,
339 net ablation of up to 10 m yr^{-1} is predicted. In MRI-CGCM2.3 (AOGCM), the cold summer Pliocene
340 temperatures (Fig. 4; Table 3) lead to accumulation over most of the landmass of Greenland (Fig. 8).
341 Conversely, the high summer temperatures exhibited in the NorESM-L models means that the GrIS
342 area experiences only ablation, even over the centre of the PRISM3 GrIS.

343 Figure 9 shows the spatial distribution of the GrIS when BASISM (standard parameter set; red dots in
344 Fig. 7) is forced with atmospheric input fields from each of the PlioMIP models. These results show
345 large differences in both the ice thickness and extent from one simulation to another. Using the
346 AGCMs, ice cover ranges from no ice (NorESM-L) to modern extent (COSMOS, MIROC4m and
347 MRI-CGCM2.3). The absence of ice in the NorESM-L reconstruction is due to the fact that summer
348 temperatures remain above freezing even when a lapse rate correction has been applied (that accounts
349 for the differences in altitude between the GCM and the ISM grid). Therefore, no ice is able to
350 survive the melt season in this simulation (Fig. 9). The ice sheet reconstructions using CAM3.1 (0.77
351 $\times 10^6 \text{ km}^3$) and LMDZ5A ($1.47 \times 10^6 \text{ km}^3$) provide ice sheets that are comparable in terms of volume
352 to the PRISM3 GrIS ($1.07 \times 10^6 \text{ km}^3$), although the distribution of ice is most similar in LMDZ5A
353 (Fig. 9).

354 All AOGCMs produce some ice over Greenland during the mPWP (Fig. 9) and seven of the eight
355 reconstructions show a reduction in volume in comparison to the GCM-specific pre-industrial
356 counterpart (Table 4). Ice is distributed in these seven reconstructions as two ice caps, one in the
357 South of Greenland and one spreading out from the mountains of East Greenland. The simulation
358 performed using MRI-CGCM2.3 (AOGCM) produces a GrIS of modern extent with an overall
359 increase in modelled volume relative to the pre-industrial control (+6.3%; Table 4). This is consistent
360 with the MRI-CGCM2.3 (AOGCM) simulated Pliocene temperature over Greenland, which is on
361 average 9°C warmer than the MRI-CGCM2.3 pre-industrial. Nevertheless, the absolute Pliocene
362 temperatures remain much colder than those simulated within the rest of the ensemble, and are
363 actually more akin to the range of pre-industrial temperatures simulated by the other models (Table
364 3). At the other extreme, NorESM-L produces a GrIS which is reduced in areal extent by 1.41×10^6
365 km^2 (equivalent to a simulated sea level increase of $>7\text{m}$). GISS ModelE2-R, HadCM3 and
366 IPSLCM5A produce relatively similar ice sheet configurations over Greenland with the Northern ice

367 cap not extending across to West Greenland. However, the ice sheets reconstructed by CCSM4,
368 COSMOS and MIROC4m either reach or stretch to within ~60 km of the Baffin Bay coastline (Fig.
369 9). In terms of areal extent and volume, the IPSLCM5A and the GISS ModelE2-R ice sheet
370 reconstructions are the closest to the original PRISM3 GrIS.

371 **4. Discussion**

372 To date, only a few studies (e.g. Charbit et al., 2007; Quiquet et al., 2012; Yan et al., 2013) have
373 explicitly tested the sensitivity of an ISM to atmospheric input fields, with more studies focussing on
374 parametric uncertainty within ice sheet modelling (e.g. Marshall et al., 2002; Tarasov and Peltier,
375 2004; Hebeler et al., 2008; Stone et al., 2010). In this study we have tested the climate model
376 dependency of ice sheet reconstructions using output from multiple Pliocene climate models. The
377 simulated realisations of the mid-Pliocene GrIS reveals significant differences from one simulation to
378 the other, with respect to both the simulated ice volume and ice-covered area, and to the shape and
379 spatial distribution of the ice sheet.

380 **4.1 Understanding Climate Model Differences**

381 By comparing the ISM output (Fig. 9) with GCM-predicted mid-Pliocene climate forcing (Figs. 2 to
382 4) and the calculated SMB fields (Fig. 8), it is clear that some of the major variations are reflected in
383 the differences in temperature and precipitation distribution amongst the model ensemble. This is in
384 agreement with the study of Charbit et al. (2007), who demonstrated that variability in climate forcing
385 through the last glacial-interglacial cycle induced large differences in simulated Northern Hemisphere
386 ice sheets.

387 In order to better understand the mechanisms that cause inter-climate model differences in
388 temperature, a more in-depth analysis is required that investigates how changes in the energy balance
389 lead to a redistribution of global heat (e.g. Heinemann et al., 2009; Lunt et al., 2012). Hill et al.
390 (2014) have performed such an analysis on the AOGCM (Experiment 2) results from PlioMIP and
391 have shown that the dominant control on annual mean temperature changes in the Arctic regions is
392 related to the clear sky albedo in each model. All AOGCM simulations show that the strongest
393 warming signals come from clear sky albedo (α), although the range in the magnitude of this warming
394 is large (3-12°C; Hill et al., 2014). Clear sky albedo reflects changes on the Earth surface such as
395 vegetation, snow cover and ice (both terrestrial ice and sea ice).

396 Figures 10 and 11 show the clear sky albedo values for the pre-industrial and mid-Pliocene
397 simulations respectively from within the entire PlioMIP ensemble. The clear sky albedo value for

398 each model is relatively similar for the pre-industrial simulations (except MRI-CGCM2.3 (AOGCM);
399 Fig. 10), although there are differences in the albedo values at the margins of the ice sheets. Whilst
400 this is sometimes linked to the resolution of the climate model giving either a finer (e.g. CCSM4
401 AOGCM) or a coarser (e.g. MRI-CGCM2.3 AOGCM) representation of albedo around Greenland, it
402 can also be attributed to the different albedo properties of snow in each of the climate models (Table
403 5). For example, some climate models have deep-snow albedo values that are dependent on
404 temperature (e.g. HadCM3, MRI-CGCM2.3 and COSMOS) but the range of maximum and minimum
405 albedo values are not always identical (e.g. the minimum albedo in COSMOS is 0.6 whereas in MRI-
406 CGCM2.3 it is 0.64). Moreover not all climate models account for factors that influence snow
407 albedo such as the aging of snow or the radiative effects of darkening snow. The differences in the
408 snow albedo schemes implemented in the ensemble may help to explain the differences shown in the
409 Pliocene experiments especially over the GrIS region (Fig. 11).

410 In the ice-free regions of Greenland prescribed in PliomIP, modelling groups were asked to
411 implement the Salzmann et al. (2008) vegetation reconstruction. Due to the challenging nature of this
412 task different implementation methods were used within the modelling groups. The vegetation
413 distribution was given to the groups in terms of the BIOME4 biome or mega-biome types (Salzmann
414 et al., 2008). However, most modelling groups were unable to implement the data set exactly and
415 instead mapped the plant-functional types onto their own biome scheme. In some cases (e.g. with the
416 GISS ModelE2-R) this meant that distinct biome types within BIOME4 became merged into broader
417 categories within an individual model scheme (Chandler et al., 2013). It is therefore likely that the
418 albedo properties of the altered vegetation types could be quite different between models, which may
419 be an important factor in the clear sky albedo differences shown in Figure 11.

420 The impact of differing albedo schemes over Greenland can be seen clearly in the MRI-CGCM2.3
421 (AOGCM) reconstruction of the mid-Pliocene GrIS (Fig. 9). The high albedo values relative to other
422 models are associated with much colder Pliocene temperatures (comparable with most pre-industrial
423 simulations; Table 3) and lead to the reconstruction of a modern-sized Pliocene GrIS (Table 4; Fig. 9).
424 High albedo values in the AOGCM version of MRI-CGCM2.3 are also consistent with results from
425 Hill et al. (2014), which show this model as having the least contribution to Pliocene warming from
426 clear sky albedo.

427 In the AOGCMs, it is also useful to consider differences in predicted sea-surface temperatures (SSTs)
428 and sea-ice around the Greenland region. Hill et al (2010) and Koenig et al. (2014) have shown
429 minimal and large responses respectively of the GrIS to fixed SSTs within a climate model. Whilst
430 these studies are not directly comparable (due to the use of different modelling frameworks and
431 different initial conditions), Hill et al. (2010) suggest that the GrIS volume is relatively insensitive to
432 changes in SSTs, with alterations in precipitation being the dominant forcing of the small changes

433 (<20% of present GrIS volume). However, Koenig et al. (2014) have demonstrated a greater
434 sensitivity of the GrIS to changes in temperature incurred by fixed SST and sea ice boundary
435 conditions in the climate model. Also, Ballantyne et al. (2013) have shown that Arctic continental
436 temperatures in general (including those over Greenland) are highly sensitive to the prescription of
437 sea-ice conditions within a model. For the AGCMs the Pliocene albedo values over the sea ice region
438 around the coast of Greenland are very similar, reflecting the prescribed sea-ice conditions in these
439 models (including a sea-ice free summer; Fig. 11; see also Haywood et al., 2010). Minor albedo
440 differences in the AGCMs are attributed to the varying sea-ice albedo schemes used in the models.
441 Conversely, in the AOGCMs, where the models can freely simulate sea ice conditions, there are
442 significant differences in albedo values which reflect the variability in sea-ice predictions in this
443 region. Howell et al. (in prep) have performed an in-depth analysis of the differences in Arctic sea-ice
444 predictions within the PlioMIP AOGCM ensemble. It is possible to draw correlations between some
445 models' sea-ice and GrIS reconstructions. For example, the higher summer temperature in July in
446 NorESM-L may be partially attributed to the greatly reduced sea-ice and increased SSTs over the sub-
447 polar North Atlantic. Whereas using CCSM4, which retains a substantial sea-ice cover in the Arctic
448 during summer, produces one of the largest predicted GrISs (Fig. 9; Howell, *pers. comm.*). Whilst the
449 differing conditions in the surrounding oceans offer some explanation as to the different GrIS
450 predictions from the PlioMIP AOGCM ensemble, they do little to shed light upon the reasons for
451 inter-model differences within the AGCMs. Thus it is difficult to promote sea-ice and SSTs as the
452 sole fundamental control on the extent of the GrIS based on the results presented here.

453 One further potential contributor to the inter-model differences between ice sheet reconstructions
454 could be the differences in resolution within the PlioMIP ensemble, as GCM resolution (within one
455 model) has been shown to impact on the simulated climate (Roeckner et al., 2006). On one hand,
456 there are multiple scenarios presented here where the GCM horizontal resolution is comparable (i.e.
457 COSMOS and NorESM-L, MIROC4m and MRI-CGCM2.3), but the simulated ice sheet is very
458 different (Fig. 9). However, it is also noticeable that the extent of the prescribed GrIS within each of
459 the PlioMIP models is slightly different due to the model resolution (Table 1). This can be seen most
460 clearly when considering the southward and eastward extent of the regions of accumulation (where
461 the model predicts a positive SMB) in Figure 8. In general such regions of positive SMB track the
462 shape of the prescribed PRISM3 ice sheet in the GCM, and the overall area of accumulation will have
463 an influence on the final GrIS volume.

464 Where possible, it is also interesting to contrast the results obtained from using a fully-coupled
465 version of the model to those obtained using the atmospheric component of the same model (Fig. 12).
466 Six model lineages can be considered in this way; COSMOS (AGCM/AOGCM, Stepanek and
467 Lohmann, 2012), HadAM3/HadCM3 (Bragg et al., 2012), LMDZ5A/IPSLCM5A (Contoux et al.,
468 2012), MIROC4m (AGCM/AOGCM, Chan et al., 2011), MRI-CGCM2.3 (AGCM/AOGCM, Kamae

469 and Ueda, 2012) and NorESM-L (AGCM/AOGCM, Zhang et al., 2012a; 2012b). As the AOGCM
470 experiments incorporate a dynamic ocean, there is no reason to anticipate that the reconstructed ice
471 sheets will necessarily be comparable when only the atmospheric component of the model is
472 employed. Of the six climate models, four simulate a larger GrIS using the AGCM component than
473 the AOGCM (COSMOS, LMDZ5A/IPSLCM5A, HadAM3/HadCM3 and MIROC4m; Fig. 9). Larger
474 ice sheets are generally associated with the decrease in summer temperatures and increase in
475 precipitation levels in the AGCMs (Fig. 12).

476 In summary, there are substantial differences in the predicted volumes of the GrIS when forced with
477 multiple climate model predictions (performing a standard experiment), which suggests that the
478 climate model dependency of ISM results is high. However, it is difficult to ascertain why the
479 modelled differences occur between the PlioMIP simulations, although we have shown that the clear
480 sky albedo within each model may be an important factor. In contrast, Koenig et al. (2014b) derive a
481 much lower inter-ISM spread when reconstructing the GrIS during the Pliocene, which suggests that
482 relative to climate model dependency, ISM dependency is low. This also gives us confidence that the
483 BASISM-based ice sheet predictions presented here would also hold true if repeated with a different
484 ISM (see also Yan et al., 2014).

485 **4.2 Understanding the Pliocene Greenland Ice Sheet**

486 Our results show a high climate model dependency of ISM simulations over Greenland, which implies
487 that the PRISM3 ice sheet configuration (Hill, 2009; Dowsett et al., 2010) is likely dependent on the
488 climate model used within the modelling framework (in this case HadAM3). A better estimation of
489 the GrIS during the mPWP might be derived from considering a ‘mean’ modelled ice sheet, rather
490 than a single reconstruction. A number of studies have shown that a multi-model average often out-
491 performs any individual model if compared to observations (Knutti et al., 2010). This has been
492 demonstrated for mean climate (Gleckler et al., 2008; Reichler and Kim, 2008), but also in regional
493 climate model assessments of the mid-Pliocene (Zhang et al., 2013). A similar approach was taken
494 for defining the Last Glacial Maximum (LGM) ice sheet configuration in the Northern Hemisphere.
495 In the PMIP3/CMIP5 LGM experiments a blended product was obtained by averaging three different
496 ice sheet reconstructions, because of the uncertainties associated with each individual reconstruction
497 (PMIP3, 2010). Here we have calculated an un-weighted multi-model mean (MMM), which is the
498 average of simulations in our multi-model ensemble, treating all models equally.

499 We have calculated MMMs for both the ice sheet configurations derived using the standard BASISM
500 glaciological parameters and the parameter sets that give the best GrIS reconstruction in terms of
501 modern volume. Figure 13a displays the differences between the calculated MMMs for the AGCM

502 and AOGCM simulations. Present-day observations suggest that if the modern GrIS entirely
503 deglaciated, global sea would rise by around 7.36 m (Bamber et al., 2013). The Pliocene GrIS MMM
504 volumes are equivalent to a range in global sea level rise of 2.2 to 4.4 m (Fig. 13a). Due to the
505 difficulties in creating a spatially consistent MMM GrIS, possible ice sheet configurations (taken from
506 the BASISM ensemble of predicted ice sheets) that are approximately equal to the largest and smallest
507 MMM volume are shown in Figure 13b. It is notable that the smallest MMM ice sheet is very similar
508 to the PRISM3 GrIS boundary condition prescribed in the PlioMIP climate models (Fig. 1), with the
509 exception of the ice cap on Southern Greenland.

510 There are nevertheless a number of problems with this approach that suggest that caution should be
511 applied when interpreting these results. Firstly, given sea level records and proximal estimates of
512 Greenland ice, it is unlikely that a modern-extent GrIS prevailed during the warmest parts of the
513 mPWP. In the case of the AOGCM ‘best-fit’ parameters, the removal of the large MRI-CGCM2.3 ice
514 sheet reconstruction would make the ensemble spread significantly smaller and also impact upon the
515 calculated MMM (the alternative MMM ice sheet reconstruction in this case would be equivalent to a
516 5.1 m sea level rise rather than 4.4 m).

517 Secondly, Contoux et al. (in review) highlight the possibility that the use of the PRISM3 GrIS as a
518 climate model boundary condition for the experiments presented here might bias or precondition the
519 subsequent ISM experiments towards a PRISM3-like GrIS. Contoux et al. (in review) show that
520 when an ice-free Greenland is prescribed in the IPSLCM5A climate model, the subsequent ISM
521 reconstruction is smaller than the PRISM3 GrIS and restricted to the East Greenland Mountains and
522 the southern tip of Greenland. This is supported by the inter-model assessment presented in Koenig et
523 al. (2014b). When prescribing an ice-free Greenland during the Pliocene in HadAM3, five SIA ISMs
524 reconstruct a mean ice loss equivalent to a ~7 m global sea level rise. However, when using the same
525 set of boundary conditions to this study (i.e. PRISM3 ice in HadAM3), the contribution of the GrIS to
526 sea level rise ranges between 2.2 m and 1.6 m as a MMM (see Koenig et al. 2014b for further details).
527 This highlights the impact of the choice of the initial ice configuration in the climate model. However,
528 without a fully coupled ice-sheet-climate model, this is a difficult problem to overcome. Given the
529 modelling framework adopted here, and the likely presence of ice on Greenland, it is essential to
530 prescribe an ice sheet in the climate model, which requires a number of *a priori* assumptions
531 regarding ice distribution. Not only does this have implications for our understanding of the GrIS
532 during warm interglacials of the Pliocene, an incorrect representation of the ice sheets in general may
533 have a negative impact when assessing global climate model simulations against proxy-data from the
534 warm Pliocene (e.g. Dowsett et al., 2012; 2013; Haywood et al., 2013; Salzmann et al., 2013).

535 A final caveat to this research is derived from the uncertainty as to whether a good simulation of the
536 modern GrIS (when compared to observations) necessarily implies a realistic representation of the

537 Pliocene GrIS. Robinson et al. (2011) found that when simulating the Eemian GrIS (where
538 significantly more constraints are available than for the Pliocene), the ISM simulation that gave the
539 most realistic modern ice sheet, gave an entirely unrealistic ice sheet for the Eemian when compared
540 with proxy data. This highlights the need for further palaeodata constraints regarding the extent and
541 thickness (where possible) of the Pliocene GrIS in order to thoroughly assess the results presented
542 here.

543 **4.3 Climate Model Boundary Conditions for PlioMIP Phase 2**

544 The final aim of this study and the wider PLISMIP project (Dolan et al., 2012) is to inform decisions
545 regarding the ice sheet boundary conditions to be prescribed in the second phase of PlioMIP
546 (Haywood et al., in prep). The high climate model dependency of the GrIS shown here now brings
547 into question the suitability of the PRISM3 GrIS in PlioMIP Phase 1, as this was the result of a one
548 climate model/one ISM modelling framework. However, the broad range in the MMM ensemble
549 presented here and the problems associated with *a priori* assumptions necessary to undertake this
550 modelling framework suggest that the simple use of a MMM GrIS is inappropriate.

551 It is therefore likely that future GrIS reconstructions will be based on a combination of climate/ice
552 sheet modelling results (e.g. Koenig et al., 2014b; Contoux et al., in review and those presented here)
553 and data-based constraints. Evidence for vegetation, suggesting ice-free conditions can be found in
554 North Greenland (Funder et al., 2001), at Ile de France (Bennike et al., 2002), on Ellesmere Island and
555 the Canadian Archipelago (De Vernal and Mudie, 1989; Thompson and Flemming, 1996; Ballantyne
556 et al., 2006; Csank et al., 2011), and these offer limited constraints on a mPWP GrIS reconstruction.
557 More recently Bierman et al. (2014) have shown a preservation of a preglacial landscape under the
558 centre of the GrIS at the site of the Greenland Ice Sheet Project 2 core. They suggest that the soils
559 which formed at the base of the core (at the onset of Northern Hemisphere Glaciation around 2.7 Ma)
560 could have been subaerially exposed for between 200,000 and 1 million years, which has been
561 suggested to imply that this region was potentially ice-free in the warm Pliocene. Additionally, a
562 recent reassessment of pollen derived from ODP Hole 646B off southwest Greenland (de Vernal and
563 Mudie, 1989) confirms that Southern Greenland would have been vegetated (boreal and cool-
564 temperate conditions) during parts of the warm Pliocene (de Vernal, pers. comm.).

565 Combined, the proxy-based evidence and the modelling work done to date would suggest that a
566 smaller ice cap (in relation to PRISM3), centred on the Eastern Greenland Mountains, is the best
567 available estimation of a warm interglacial Pliocene GrIS configuration. Clearly however, there is a
568 critical need for further data pertaining to ice extent (e.g. Bierman et al., 2014) or potentially the

569 Greenland climate (such as vegetation records) in order to more accurately constrain this
570 reconstruction.

571 **5. Conclusions**

572 The Pliocene Ice Sheet Modelling Intercomparison Project (Dolan et al., 2012) was initiated in order
573 to ascertain the degree to which ice predictions over Greenland are influenced by the choice of ISM
574 and climate model. Whilst Koenig et al. (2014b) have shown that ISMs are generally relatively
575 consistent in their predictions when forced with the same climatology, here we show that the choice of
576 climate model significantly affects the predicted GrIS. Ice sheet reconstructions using forcing from
577 the PlioMIP AGCMs and AOGCMs range from a larger-than-modern GrIS to an ice-free Greenland.
578 Such a result demonstrates the difficulty in using only one climate model to draw conclusions
579 regarding ice sheet stability in the warm Pliocene and highlights the need for an alternative ice sheet
580 reconstruction going forward with PlioMIP Phase 2.

581 **Acknowledgements**

582 A.M.D., S.J.H. and A.M.H. acknowledge that the research leading to these results has received
583 funding from the European Research Council under the European Union's Seventh Framework
584 Programme (FP7/2007-2013)/ERC grant agreement no. 278636. A.M.D. also acknowledges the
585 Natural Environment Research Council (NERC) for the receipt of a doctoral training grant. D.J.H.
586 acknowledges the Leverhulme Trust for the award of an Early Career Fellowship and the National
587 Centre for Atmospheric Science and the British Geological Survey for financial support. S.J.K was
588 supported by the US National Science Foundation under the awards ATM-0513402, AGS-1203910
589 and OCE-1202632. D.J.L and F.J.B. acknowledge NERC grant NE/H006273/1. The HadCM3
590 simulations were carried out using the computational facilities of the Advanced Computing Research
591 Centre, University of Bristol – <http://www.bris.ac.uk/acrc/>. G. L. received funding through the
592 Helmholtz research programme PACES and the Helmholtz Climate Initiative REKLIM. C. S.
593 acknowledges financial support from the Helmholtz Graduate School for Polar and Marine Research
594 and from REKLIM. Funding for L.S. and M.C. provided by NSF Grant ATM0323516 and NASA
595 Grant NNX10AU63A. B.L.O. and N.A.R. recognise that NCAR is sponsored by the US National
596 Science Foundation (NSF), this work was also supported through grant NSF-EAR-1237211, and
597 computing resources were provided by the Climate Simulation Laboratory at NCAR's Computational
598 and Information Systems Laboratory (CISL), sponsored by the NSF and other agencies. W.-L.C. and
599 A.A.-O. would like to thank the Japan Society for the Promotion of Science for financial support and
600 R. Ohgaito for advice on setting up the MIROC4m experiments on the Earth Simulator, JAMSTEC.

601 The source code of MRI-CGCM2.3 model is provided by S. Yukimoto, O. Arakawa, and A. Kitoh in
602 Meteorological Research Institute, Japan. Z.Z. acknowledges that the development of NorESM-L was
603 supported by the Earth System Modelling (ESM) project funded by Statoil, Norway. We also thank
604 Richard Hindmarsh of the British Antarctic Survey for the use of BASISM.

605 **References**

- 606 Ballantyne, A. P., Rybczynski, N., Baker, P. A., Harington, C. R., and White, D.: Pliocene Arctic
607 temperature constraints from the growth rings and isotopic composition of fossil larch,
608 *Palaeogeography, Palaeoclimatology, Palaeoecology*, 242, 188-200, 2006.
- 609 Ballantyne, A. P., Greenwood, D. R., Sinninghe Damsté, J. S., Csank, A. Z., Eberle, J. J., and
610 Rybczynski, N.: Significantly warmer Arctic surface temperatures during the Pliocene indicated by
611 multiple independent proxies, *Geology*, 38, 603-606, 10.1130/g30815.1, 2010.
- 612 Ballantyne, A. P., Axford, Y., Miller, G. H., Otto-Bliesner, B. L., Rosenbloom, N., and White, J. W.
613 C.: The amplification of Arctic terrestrial surface temperatures by reduced sea-ice extent during
614 the Pliocene, *Palaeogeography, Palaeoclimatology, Palaeoecology*, 386, 59-67,
615 <http://dx.doi.org/10.1016/j.palaeo.2013.05.002>, 2013.
- 616 Bamber, J. L., Ekholm, S., and Krabill, W. B.: A new, high-resolution digital elevation model of
617 Greenland fully validated with airborne laser altimeter data, *J. Geophys. Res.*, 106, 6733-6745,
618 10.1029/2000jb900365, 2001.
- 619 Bamber, J. L., Griggs, J. A., Hurkmans, R. T. W. L., Dowdeswell, J. A., Gogineni, S. P., Howat, I.,
620 Mouginot, J., Paden, J., Palmer, S., Rignot, E., and Steinhage, D.: A new bed elevation dataset for
621 Greenland, *The Cryosphere*, 7, 499-510, 10.5194/tc-7-499-2013, 2013.
- 622 Bartoli, G., Honisch, B., and Zeebe, R. E.: Atmospheric CO₂ decline during the Pliocene
623 intensification of Northern Hemisphere glaciations, *Paleoceanography*, 26, PA4213
624 10.1029/2010pa002055, 2011.
- 625 Bennike, O., Abrahamsen, N., Bak, M., Israelson, C., Konradi, P., Matthiessen, J., and Witkowski, A.:
626 A multi-proxy study of Pliocene sediments from Île de France, North-East Greenland,
627 *Palaeogeography, Palaeoclimatology, Palaeoecology*, 186, 1-23, 10.1016/S0031-0182(02)00439-
628 X, 2002.

629 Bierman, P. R., Corbett, L. B., Graly, J. A., Neumann, T. A., Lini, A., Crosby, B. T., and Rood, D. H.:
630 Preservation of a Preglacial Landscape Under the Center of the Greenland Ice Sheet, *Science*,
631 10.1126/science.1249047, 344 (6182), 402-405, 2014.

632 Born, A., and Nisancioglu, K. H.: Melting of Northern Greenland during the last interglaciation, *The*
633 *Cryosphere*, 6, 1239-1250, 10.5194/tc-6-1239-2012, 2012.

634 Braconnot, P., Harrison, S. P., Kageyama, M., Bartlein, P. J., Masson-Delmotte, V., Abe-Ouchi, A.,
635 Otto-Bliesner, B., and Zhao, Y.: Evaluation of climate models using palaeoclimatic data, *Nature*
636 *Clim. Change*, 2, 417-424, 2012.

637 Bragg, F. J., Lunt, D. J., and Haywood, A. M.: Mid-Pliocene climate modelled using the UK Hadley
638 Centre Model: PlioMIP Experiments 1 and 2, *Geosci. Model Dev.*, 5, 1109-1125, 10.5194/gmd-5-
639 1109-2012, 2012.

640 Braithwaite, R. J.: Positive degree-day factors for ablation on the Greenland ice sheet studied by
641 energy-balance modelling., *Journal of Glaciology*, 41, 153-160, 1995.

642 Chan, W. L., Abe-Ouchi, A., and Ohgaito, R.: Simulating the mid-Pliocene climate with the MIROC
643 general circulation model: experimental design and initial results, *Geosci. Model Dev.*, 4, 1035-
644 1049, 10.5194/gmd-4-1035-2011, 2011.

645 Chandler, M. A., Sohl, L. E., Jonas, J. A., Dowsett, H. J., and Kelley, M.: Simulations of the mid-
646 Pliocene Warm Period using two versions of the NASA/GISS ModelE2-R Coupled Model,
647 *Geosci. Model Dev.*, 6, 517-531, 10.5194/gmd-6-517-2013, 2013.

648 Charbit, S., Ritz, C., and Ramstein, G.: Simulations of Northern Hemisphere ice-sheet retreat::
649 sensitivity to physical mechanisms involved during the Last Deglaciation, *Quaternary Science*
650 *Reviews*, 21, 243-265, 10.1016/s0277-3791(01)00093-2, 2002.

651 Charbit, S., Ritz, C., Philippon, G., Peyaud, V., and Kageyama, M.: Numerical reconstructions of the
652 Northern Hemisphere ice sheets through the last glacial-interglacial cycle, *Clim. Past*, 3, 15-37,
653 10.5194/cp-3-15-2007, 2007.

654 Church, J.A., Clark P.U., Cazenave A., Gregory J.M., Jevrejeva S., Levermann A., Merrifield M.A.,
655 Milne G.A., Nerem R.S., Nunn P.D., Payne A.J., Pfeffer W.T., Stammer D. and Unnikrishnan
656 A.S., 2013: Sea Level Change. In: *Climate Change 2013: The Physical Science Basis.*
657 *Contribution of Working Group I to the Fifth Assessment Report of the Intergovernmental Panel*
658 *on Climate Change* [Stocker, T.F., D. Qin, G.-K. Plattner, M. Tignor, S.K. Allen, J. Boschung, A.
659 Nauels, Y. Xia, V. Bex and P.M. Midgley (eds.)]. Cambridge University Press, Cambridge, United
660 Kingdom and New York, NY, USA.

661 Collins, W. D., Rasch, P. J., Boville, B. A., Hack, J. J., McCaa, J. R., Williamson, D. L., Kiehl, J. T.,
662 and Briegleb, B.: Description of the NCAR Community Atmosphere Model (CAM 3.0), National
663 Center For Atmospheric Research, Boulder, Colorado, Climate And Global Dynamics Division,
664 2004.

665 Contoux, C., Ramstein, G., and Jost, A.: Modelling the mid-Pliocene Warm Period climate with the
666 IPSL coupled model and its atmospheric component LMDZ5A, *Geosci. Model Dev.*, 5, 903-917,
667 10.5194/gmd-5-903-2012, 2012.

668 Contoux, C., Dumas, C., Ramstein, G., Jost, A., and Dolan, A. M.: Modelling Greenland Ice sheet
669 inception and sustainability during the late Pliocene, *Earth and Planetary Sci. Lett.*, in review.

670 Cox, P. M., Betts, R. A., Bunton, C. B., Essery, R. L. H., Rowntree, P. R., and Smith, J.: The impact
671 of new land surface physics on the GCM simulation of climate and climate sensitivity, *Climate
672 Dynamics*, 15, 183-203, 10.1007/s003820050276, 1999.

673 Csank, A. Z., Tripathi, A. K., Patterson, W. P., Eagle, R. A., Rybczynski, N., Ballantyne, A. P., and
674 Eiler, J. M.: Estimates of Arctic land surface temperatures during the early Pliocene from two
675 novel proxies, *Earth and Planetary Science Letters*, 304, 291-299, 10.1016/j.epsl.2011.02.030,
676 2011.

677 Cuffey, K. M., and Marshall, S. J.: Substantial contribution to sea-level rise during the last interglacial
678 from the Greenland ice sheet, *Nature*, 404, 591-594, 2000.

679 Dahl-Jensen, D., Mosegaard, K., Gundestrup, N., Clow, G. D., Johnsen, S. J., Hansen, A. W., and
680 Balling, N.: Past Temperatures Directly from the Greenland Ice Sheet, *Science*, 282, 268-271,
681 10.1126/science.282.5387.268, 1998.

682 de Vernal, A., and Mudie, P. J.: Pliocene and Pleistocene Palynostratigraphy at ODP Sites 646 and
683 647, Eastern and Southern Labrador Sea, 401-422, 1989.

684 DeConto, R. M., and Pollard, D.: A coupled climate-ice sheet modeling approach to the Early
685 Cenozoic history of the Antarctic ice sheet, *Palaeogeography, Palaeoclimatology, Palaeoecology*,
686 198, 39-52, 10.1016/s0031-0182(03)00393-6, 2003.

687 Dolan, A. M., Haywood, A. M., Hill, D. J., Dowsett, H. J., Hunter, S. J., Lunt, D. J., and Pickering, S.
688 J.: Sensitivity of Pliocene ice sheets to orbital forcing, *Palaeogeography, Palaeoclimatology,
689 Palaeoecology*, 309, 98-110, 10.1016/j.palaeo.2011.03.030, 2011.

690 Dolan, A. M., Koenig, S. J., Hill, D. J., Haywood, A. M., and DeConto, R. M.: Pliocene Ice Sheet
691 Modelling Intercomparison Project (PLISMIP) – experimental design, *Geosci. Model Dev.*, 5,
692 963-974, 10.5194/gmd-5-963-2012, 2012.

693 Dowsett, H. J., Barron, J. A., Poore, R. Z., Thompson, R. S., Cronin, T. M., Ishman, S. E., and
694 Willard, D. A.: Middle Pliocene Paleoenvironmental Reconstruction: PRISM 2, U.S. Geological
695 Survey, Open File Report, 99-535, 1999.

696 Dowsett, H. J., Robinson, M. M., Haywood, A. M., Salzmann, U., Hill, D. J., Sohl, L. E., Chandler,
697 M., Williams, M., Foley, K., and Stoll, D. K.: The PRISM3D paleoenvironmental reconstruction.,
698 *Stratigraphy*, 7, 123-139, 2010. Dowsett, H. J., Robinson, M. M., Haywood, A. M., Hill, D. J.,
699 Dolan, A. M., Stoll, D. K., Chan, W.-L., Abe-Ouchi, A., Chandler, M. A., Rosenbloom, N. A.,
700 Otto-Bliesner, B. L., Bragg, F. J., Lunt, D. J., Foley, K. M., and Riesselman, C. R.: Assessing
701 confidence in Pliocene sea surface temperatures to evaluate predictive models, *Nature Climate*
702 *Change*, 2, 365–371 doi:10.1038/nclimate1455, 2012.

703 Dowsett, H. J., Foley, K. M., Stoll, D. K., Chandler, M. A., Sohl, L. E., Bentsen, M., Otto-Bliesner, B.
704 L., Bragg, F. J., Chan, W.-L., Contoux, C., Dolan, A. M., Haywood, A. M., Jonas, J. A., Jost, A.,
705 Kamae, Y., Lohmann, G., Lunt, D. J., Nisancioglu, K. H., Abe-Ouchi, A., Ramstein, G.,
706 Riesselman, C. R., Robinson, M. M., Rosenbloom, N. A., Salzmann, U., Stepanek, C., Strother, S.
707 L., Ueda, H., Yan, Q., and Zhang, Z.: Sea Surface Temperature of the mid-Piacenzian Ocean: A
708 Data-Model Comparison, *Nature Sci. Rep.*, 3, 10.1038/srep02013, 2013.

709 Ebert, E. E., and Curry, J. A.: An intermediate one-dimensional thermodynamic sea ice model for
710 investigating ice-atmosphere interactions, *Journal of Geophysical Research*, 98, 10085–10109,
711 1993.

712 Flanner, M. G., and Zender, C. S.: Linking snowpack microphysics and albedo evolution, *Journal of*
713 *Geophysical Research: Atmospheres*, 111, D12208, 10.1029/2005jd006834, 2006.

714 Funder, S., Bennike, O., Böcher, J., Israelson, C., Petersen, K. S., and Símonarson, L. A.: Late
715 Pliocene Greenland - The Kap København Formation in North Greenland, *Bulletin of the*
716 *Geological Society of Denmark*, 48, 117-134, 2001.

717 Gent, P. R., Danabasoglu, G., Donner, L. J., Holland, M. M., Hunke, E. C., Jayne, S. R., Lawrence, D.
718 M., Neale, R. B., Rasch, P. J., Vertenstein, M., Worley, P. H., Yang, Z.-L., and Zhang, M.: The
719 Community Climate System Model Version 4, *Journal of Climate*, 24, 4973-4991,
720 10.1175/2011jcli4083.1, 2011.

721 Gleckler, P. J., Taylor, K. E., and Doutriaux, C.: Performance metrics for climate models, *Journal of*
722 *Geophysical Research: Atmospheres*, 113, D06104, 10.1029/2007jd008972, 2008.

723 Hanna, E., Huybrechts, P., Janssens, I., Cappelen, J., Steffen, K., and Stephens, A.: Runoff and mass
724 balance of the Greenland ice sheet, *J. Geophys. Res.*, 110, 10.1029/2004jd005641, D13108, 2005.

725 Haywood, A. M., Valdes, P. J., and Sellwood, B. W.: Global scale palaeoclimate reconstruction of the
726 middle Pliocene climate using the UKMO GCM: initial results, *Global and Planetary Change*, 25,
727 239-256, 10.1016/S0921-8181(00)00028-X, 2000.

728 Haywood, A. M., Chandler, M. A., Valdes, P. J., Salzmann, U., Lunt, D. J., and Dowsett, H. J.:
729 Comparison of mid-Pliocene climate predictions produced by the HadAM3 and GCMAM3
730 General Circulation Models, *Global and Planetary Change*, 66, 208-224,
731 10.1016/j.gloplacha.2008.12.014, 2009.

732 Haywood, A. M., Dowsett, H. J., Otto-Bliesner, B., Chandler, M., Dolan, A., Hill, D. J., Lunt, D. J.,
733 Robinson, M. M., Rosenbloom, N., Salzmann, U., and Sohl, L. E.: Pliocene Model
734 Intercomparison Project (PlioMIP): Experimental Design & Boundary Conditions (Experiment 1),
735 *Geoscientific Model Development*, 3, 227-242, 2010.

736 Haywood, A. M., Dowsett, H. J., Robinson, M. M., Stoll, D. K., Dolan, A. M., Lunt, D. J., Otto-
737 Bleisner, B., and Chandler, M.: Pliocene Model Intercomparison Project (PlioMIP): experimental
738 design and boundary conditions (Experiment 2), *Geoscientific Model Development* 4, 571-577,
739 doi:10.5194/gmd-4-571-2011, 2011.

740 Haywood, A. M., Hill, D. J., Dolan, A. M., Otto-Bliesner, B. L., Bragg, F., Chan, W. L., Chandler, M.
741 A., Contoux, C., Dowsett, H. J., Jost, A., Kamae, Y., Lohmann, G., Lunt, D. J., Abe-Ouchi, A.,
742 Pickering, S. J., Ramstein, G., Rosenbloom, N. A., Salzmann, U., Sohl, L., Stepanek, C., Ueda, H.,
743 Yan, Q., and Zhang, Z.: Large-scale features of Pliocene climate: results from the Pliocene Model
744 Intercomparison Project, *Clim. Past*, 9, 191-209, 10.5194/cp-9-191-2013, 2013.

745 Haywood, A. M., Dolan, A. M., Dowsett, H. J., Abe-Ouchi, A., Otto-Bleisner, B., Chandler, M., Lunt,
746 D. J., Rowley, D. B., Salzmann, U., and Pound, M. J.: The Pliocene Model Intercomparison
747 Project (PlioMIP) Phase 2: Scientific Objectives and Experimental Design, *Clim. Past.*, in prep.

748 Hebel, F., Purves, R. S., and Jamieson, S. S. R.: The impact of parametric uncertainty and
749 topographic error in ice-sheet modelling, *Journal of Glaciology*, 54, 899-919,
750 10.3189/002214308787779852, 2008.

751 Heinemann, M., Jungclaus, J. H., and Marotzke, J.: Warm Paleocene/Eocene climate as simulated in
752 ECHAM5/MPI-OM, *Clim. Past*, 5, 785-802, 10.5194/cp-5-785-2009, 2009.

- 753 Hill, D. J., Haywood, A. M., Hindmarsh, R. C. M., and Valdes, P. J.: Characterizing ice sheets during
754 the Pliocene: evidence from data and models, in: Deep-Time Perspectives on Climate Change:
755 Marrying the signal from Computer Models and Biological Proxies, edited by: Williams, M.,
756 Haywood, A. M., Gregory, F. J., and Schmidt, D. N., The Micropalaeontological Society, Special
757 Publications. The Geological Society, London, 517-538, 2007.
- 758 Hill, D. J.: Modelling Earth's Cryosphere during peak Pliocene warmth, Ph.D. Thesis, Ph. D. Thesis,
759 Ph. D. Thesis, University of Bristol, 368 pp., 2009.
- 760 Hill, D. J., Dolan, A. M., Haywood, A. M., Hunter, S. J., and Stoll, D. K.: Sensitivity of the Greenland
761 Ice Sheet to Pliocene sea surface temperatures, *Stratigraphy*, 7, 111-122, 2010.
- 762 Hill, D. J., Csank, A. Z., Dolan, A. M., and Lunt, D. J.: Pliocene climate variability: Northern Annular
763 Mode in models and tree-ring data, *Palaeogeography, Palaeoclimatology, Palaeoecology*, 309,
764 118-127, 2011.
- 765 Hill, D. J., Haywood, A. M., Lunt, D. J., Hunter, S. J., Bragg, F. J., Contoux, C., Stepanek, C., Sohl,
766 L., Rosenbloom, N. A., Chan, W. L., Kamae, Y., Zhang, Z., Abe-Ouchi, A., Chandler, M. A., Jost,
767 A., Lohmann, G., Otto-Bliesner, B. L., Ramstein, G., and Ueda, H.: Evaluating the dominant
768 components of warming in Pliocene climate simulations, *Clim. Past*, 10, 79-90, 10.5194/cp-10-79-
769 2014, 2014.
- 770 Hindmarsh, R. C. A.: Modeling the Dynamics of Ice Sheets, *Progress in Physical Geography*, 17,
771 1993.
- 772 Hindmarsh, R. C. A.: Stability of ice-rises and uncoupled marine ice sheets, *Annals of Glaciology*, 23,
773 105-115, 1996.
- 774 Hindmarsh, R. C. A.: On the numerical computation of temperature in an ice-sheet, *Journal of*
775 *Glaciology*, 45, 568-574, 1999. Hindmarsh, R. C. A.: Influence of Channelling on Heating in Ice-
776 Sheet Flows, *Geophys. Res. Lett.*, 28 (19), 3681-3684, DOI: 10.1029/2000GL012666, 2001.
- 777
- 778 Howell, F. W., Haywood, A. M., Otto-Bleisner, B., Abe-Ouchi, A., Bragg, F., Chan, W. L., Chandler,
779 M., Contoux, C., Jost, A., Kamae, Y., Lohmann, G., Lunt, D. J., Ramstein, G., Rosenbloom, N.,
780 Sohl, L., Stepanek, C., Ueda, H., Yan, Q., and Zhang, Z. S.: Simulation of sea ice in the PlioMIP
781 ensemble, in prep for *Clim. Dyn.*
- 782 Huybrechts, P.: A 3-D model for the Antarctic ice sheet: a sensitivity study on the glacial-interglacial
783 contrast, *Climate Dynamics*, 5, 79-92, 1990.

784 Huybrechts, P., Letreguilly, A., and Reeh, N.: The Greenland ice sheet and greenhouse warming,
785 *Global and Planetary Change*, 3, 399-412, 10.1016/0921-8181(91)90119-h, 1991.

786 Huybrechts, P., and de Wolde, J.: The Dynamic Response of the Greenland and Antarctic Ice Sheets
787 to Multiple-Century Climatic Warming, *Journal of Climate*, 12, 2169-2188, 1999.

788 Janssens, I., and Huybrechts, P.: The treatment of meltwater retardation in mass-balance
789 parameterizations of the Greenland Ice Sheet. *Annals of Glaciology*, 31, 133-140, 2000.

790 Johnsen, S. J., Dahl-Jensen, D., Gundestrup, N., Steffensen, J. P., Clausen, H. B., Miller, H., Masson-
791 Delmotte, V., Sveinbjörnsdóttir, A. E., and White, J.: Oxygen isotope and palaeotemperature
792 records from six Greenland ice-core stations: Camp Century, Dye-3, GRIP, GISP2, Renland and
793 NorthGRIP, *Journal of Quaternary Science*, 16, 299-307, 10.1002/jqs.622, 2001.

794 Kamae, Y., and Ueda, H.: Mid-Pliocene global climate simulation with MRI-CGCM2.3: set-up and
795 initial results of PliomIP Experiments 1 and 2, *Geosci. Model Dev.*, 5, 793-808, 10.5194/gmd-5-
796 793-2012, 2012.

797 Knutti, R., Furrer, R., Tebaldi, C., Cermak, J., and Meehl, G. A.: Challenges in Combining
798 Projections from Multiple Climate Models, *Journal of Climate*, 23, 2739-2758,
799 10.1175/2009jcli3361.1, 2010.

800 Koenig, S., DeConto, R., and Pollard, D.: Late Pliocene to Pleistocene sensitivity of the Greenland Ice
801 Sheet in response to external forcing and internal feedbacks, *Climate Dynamics*, 37, 1247-1268,
802 10.1007/s00382-011-1050-0, 2011.Koenig, S. J., DeConto, R. M., and Pollard, D.: Impact of
803 reduced Arctic sea ice on Greenland ice sheet variability in a warmer than present climate,
804 *Geophysical Research Letters*, DOI: 10.1002/2014GL059770, 41 (11), 3933–3942, 2014a.

805
806 Koenig, S.J., Dolan, A.M., de Boer, B., Stone, E.J., Hill, D.J., DeConto, R.M., Abe-Ouchi, A., Lunt,
807 D.J., Pollard, D., Quiquet, A., Saito, F and Savage, J.: Greenland Ice Sheet Sensitivity and Sea
808 Level Contribution to the mid-Pliocene Warm Period, *Climate of the Past Discussions*, 2014b.

809 Krinner, G., Viovy, N., de Noblet-Ducoudré, N., Ogée, J., Polcher, J., Friedlingstein, P., Ciais, P.,
810 Sitch, S., and Prentice, I. C.: A dynamic global vegetation model for studies of the coupled
811 atmosphere-biosphere system, *Global Biogeochemical Cycles*, 19, GB1015,
812 10.1029/2003gb002199, 2005.

813 Lawrence, D. M., Oleson, K. W., Flanner, M. G., Thornton, P. E., Swenson, S. C., Lawrence, P. J.,
814 Zeng, X., Yang, Z.-L., Levis, S., Sakaguchi, K., Bonan, G. B., and Slater, A. G.: Parameterization

815 improvements and functional and structural advances in version 4 of the Community Land Model,
816 J. Adv. Model. Earth Sys., 3, 27 pp., doi:10.1029/2011MS000045, 2011.

817 Le Meur, E., Huybrechts, P.: A comparison of different ways of dealing with isostasy: examples of
818 modelling the Antarctic Ice Sheet during the last glacial cycle, *Annals of Glaciology*, 23, 309-317,
819 1996.

820 Loth, B., and Graf, H.-F.: Modeling the snow cover in climate studies: 1. Long-term integrations
821 under different climatic conditions using a multilayered snow-cover model, *Journal of Geophysical*
822 *Research: Atmospheres*, 103, 11313-11327, 10.1029/97jd01411, 1998.

823 Lunt, D. J., Foster, G. L., Haywood, A. M., and Stone, E. J.: Late Pliocene Greenland glaciation
824 controlled by a decline in atmospheric CO₂ levels, *Nature*, 454, 1102-1105, 10.1038/nature07223,
825 2008a.

826 Lunt, D. J., Valdes, P. J., Haywood, A. M., and Rutt, I. C.: Closure of the Panama Seaway during the
827 Pliocene: implications for climate and Northern Hemisphere glaciation, *Climate Dynamics*, 30, 1-
828 18, 10.1007/s00382-007-0265-6, 2008b.

829 Lunt, D. J., Haywood, A. M., Foster, G. L., and Stone, E. J.: The Arctic cryosphere in the Mid-
830 Pliocene and the future, *Philosophical Transactions of the Royal Society, A*, 367, 49-67,
831 10.1098/rsta.2008.0218, 2009.

832 Lunt, D. J., Haywood, A. M., Schmidt, G. A., Salzmann, U., Valdes, P. J., and Dowsett, H. J.: Earth
833 system sensitivity inferred from Pliocene modelling and data, *Nature Geosci*, 3, 60-64, 2010.

834 Lunt, D. J., Haywood, A. M., Schmidt, G. A., Salzmann, U., Valdes, P. J., Dowsett, H. J., and
835 Loftson, C. A.: On the causes of mid-Pliocene warmth and polar amplification, *Earth and*
836 *Planetary Science Letters*, 321-322, 128-138, 10.1016/j.epsl.2011.12.042, 2012.

837 Marshall, S. J., James, T. S., and Clarke, G. K. C.: North American Ice Sheet reconstructions at the
838 Last Glacial Maximum, *Quaternary Science Reviews*, 21, 175-192, 10.1016/s0277-
839 3791(01)00089-0, 2002.

840 Masson-Delmotte, V., M. Schulz, A. Abe-Ouchi, J. Beer, A. Ganopolski, J.F. González Rouco, E.
841 Jansen, K. Lambeck, J. Luterbacher, T. Naish, T. Osborn, B. Otto-Bliesner, T. Quinn, R. Ramesh,
842 M. Rojas, X. Shao and A. Timmermann, 2013: Information from Paleoclimate Archives. In:
843 *Climate Change 2013: The Physical Science Basis. Contribution of Working Group I to the Fifth*
844 *Assessment Report of the Intergovernmental Panel on Climate Change* [Stocker, T.F., D. Qin, G.-
845 K. Plattner, M. Tignor, S.K. Allen, J. Boschung, A. Nauels, Y. Xia, V. Bex and P.M. Midgley

846 (eds.]. Cambridge University Press, Cambridge, United Kingdom and New York, NY, USA, 383 -
847 464.

848 Mayewski, P. A., Meeker, L. D., Whitlow, S., Twickler, M. S., Morrison, M. C., Bloomfield, P.,
849 Bond, G. C., Alley, R. B., Gow, A. J., Meese, D. A., Grootes, P. M., Ram, M., Taylor, K. C., and
850 Wumkes, W.: Changes in atmospheric circulation and ocean ice cover over the North Atlantic
851 during the last 41,000 years, *Science*, 263, 1747-1751, 1994.

852 Miller, K. G., Wright, J. D., Browning, J. V., Kulpecz, A., Kominz, M., Naish, T. R., Cramer, B. S.,
853 Rosenthal, Y., Peltier, W. R., and Sosdian, S.: High tide of the warm Pliocene: Implications of
854 global sea level for Antarctic deglaciation, *Geology*, 40, 407-410, 10.1130/g32869.1, 2012.

855 Numaguti, A., Takahashi, M., Nakajima, T., and Sumi, A.: Description of CCSR/NIES Atmospheric
856 General Circulation Model, CGERs, National Institute for Environmental Studies, Center for
857 Global Environment Research, 1-48, 1997.

858 Ohmura, A.: Physical Basis for the Temperature-Based Melt-Index Method, *Journal of Applied*
859 *Meteorology*, 40, 753-761, 10.1175/1520-0450(2001)040<0753:pbfttb>2.0.co;2, 2001.

860 Otto-Bliesner, B. L., Marshall, S. J., Overpeck, J. T., Miller, G. H., Hu, A., and CAPE Last
861 Interglacial Project members: Simulating Arctic Climate Warmth and Icefield Retreat in the Last
862 Interglaciation, *Science*, 311, 1751-1753, 2006.

863 Overpeck, J. T., Otto-Bliesner, B. L., Miller, G. H., Muhs, D. R., Alley, R. B., and Kiehl, J. T.:
864 Paleoclimatic Evidence for Future Ice-Sheet Instability and Rapid Sea-Level Rise, *Science*, 311,
865 1747-1750, 10.1126/science.1115159, 2006.

866 Pagani, M., Liu, Z., LaRiviere, J., and Ravelo, A. C.: High Earth-system climate sensitivity
867 determined from Pliocene carbon dioxide concentrations, *Nature Geosci*, 3, 27-30,
868 10.1038/ngeo724, 2010.

869 Paleoclimate Modelling Intercomparison Project Phase III: Ice Sheet for PMIP3/CMIP5 simulations,
870 available at: <https://wiki.lsce.ipsl.fr/pmip3/doku.php/pmip3:design:pi:final:icesheet>, last access: 14
871 July 2014, 2010.

872 Quiquet, A., Punge, H. J., Ritz, C., Fettweis, X., Kageyama, M., Krinner, G., Salas y Méliá, D., and
873 Sjolte, J.: Large sensitivity of a Greenland ice sheet model to atmospheric forcing fields, *The*
874 *Cryosphere Discuss.*, 6, 1037-1083, 10.5194/tcd-6-1037-2012, 2012.

875 Quiquet, A., Ritz, C., Punge, H. J., and Salas y Méliá, D.: Greenland ice sheet contribution to sea
876 level rise during the last interglacial period: a modelling study driven and constrained by ice core
877 data, *Clim. Past*, 9, 353-366, 10.5194/cp-9-353-2013, 2013.

878 Rasmussen, S. O., Andersen, K. K., Svensson, A. M., Steffensen, J. P., Vinther, B. M., Clausen, H.
879 B., Siggaard-Andersen, M. L., Johnsen, S. J., Larsen, L. B., Dahl-Jensen, D., Bigler, M.,
880 Röthlisberger, R., Fischer, H., Goto-Azuma, K., Hansson, M. E., and Ruth, U.: A new Greenland
881 ice core chronology for the last glacial termination, *Journal of Geophysical Research:
882 Atmospheres*, 111, D06102, 10.1029/2005jd006079, 2006.

883 Reeh, N.: Parameterization of melt rate and surface temperature on the Greenland ice sheet
884 *Polarforschung*, 59, 113-128, 1991.

885 Reichler, T., and Kim, J.: How Well Do Coupled Models Simulate Today's Climate?, *Bulletin of the
886 American Meteorological Society*, 89, 303-311, 10.1175/bams-89-3-303, 2008.

887 Ridley, J. K., Huybrechts, P., Gregory, J. M., and Lowe, J. A.: Elimination of the Greenland Ice Sheet
888 in a High CO₂ Climate, *Journal of Climate*, 18, 3409-3427, 10.1175/JCLI3482.1, 2005.

889 Ritz, C., Fabre, A., and Letréguilly.: Sensitivity of a Greenland ice sheet model to ice flow and
890 ablation parameters: consequences for the evolution through the last climatic cycle, *Climate
891 Dynamics*, 13, 11-24, 1997.

892 Ritz, C., Rommelaere, V., and Dumas, C.: Modeling the evolution of Antarctic ice sheet over the last
893 420,000 years: Implications for altitude changes in the Vostok region, *J. Geophys. Res.*, 106,
894 31943-31964, 10.1029/2001jd900232, 2001.

895 Robinson, A., Calov, R., and Ganopolski, A.: Greenland ice sheet model parameters constrained using
896 simulations of the Eemian Interglacial, *Clim. Past*, 7, 381-396, 10.5194/cp-7-381-2011, 2011.

897 Roeckner, E., Brokopf, R., Esch, M., Giorgetta, M., Hagemann, S., Kornbluh, L., Manzini, E.,
898 Schlese, U., and Schulzweida, U.: Sensitivity of Simulated Climate to Horizontal and Vertical
899 Resolution in the ECHAM5 Atmosphere Model, *Journal of Climate*, 19, 3771-3791,
900 10.1175/jcli3824.1, 2006.

901 Rohling, E. J., Foster, G. L., Grant, K. M., Marino, G., Roberts, A. P., Tamisiea, M. E., and Williams,
902 F.: Sea-level and deep-sea-temperature variability over the past 5.3 million years, *Nature*, 508,
903 477-482, 10.1038/nature13230, 2014.

904 Rosenbloom, N. A., Otto-Bliesner, B. L., Brady, E. C., and Lawrence, P. J.: Simulating the mid-
905 Pliocene Warm Period with the CCSM4 model, *Geosci. Model Dev.*, 6, 549-561, 10.5194/gmd-6-
906 549-2013, 2013.

907 Rovere, A., Raymo, M. E., Mitrovica, J. X., Hearty, P. J., O’Leary, M. J. and Inglis, J. D., 2014. The
908 Mid-Pliocene sea-level conundrum: Glacial isostasy, eustasy and dynamic topography, *Earth and*
909 *Planetary Science Letters*, 387, 27–33Rutt, I. C., Hagdorn, M., Hulton, N. R. J., and Payne, A. J.:
910 The Glimmer community ice sheet model, *J. Geophys. Res.*, F02004, doi:10.1029/2008JF001015,
911 114, 2009.

912
913 Saito, F., and Abe-Ouchi, A.: Sensitivity of Greenland ice sheet simulation to the numerical procedure
914 employed for ice-sheet dynamics, *Annals of Glaciology*, 42, 331-336,
915 10.3189/172756405781813069, 2005.

916 Salzmann, U., Haywood, A. M., Lunt, D. J., Valdes, P. J., and Hill, D. J.: A new global biome
917 reconstruction and data-model comparison for the Middle Pliocene, *Global Ecology and*
918 *Biogeography*, 17, 432-447, 10.1111/j.1466-8238.2008.00381.x, 2008.

919 Salzmann, U., Dolan, A. M., Haywood, A. M., Chan, W.-L., Voss, J., Hill, D. J., Abe-Ouchi, A.,
920 Otto-Bliesner, B., Bragg, F. J., Chandler, M. A., Contoux, C., Dowsett, H. J., Jost, A., Kamae, Y.,
921 Lohmann, G., Lunt, D. J., Pickering, S. J., Pound, M. J., Ramstein, G., Rosenbloom, N. A., Sohl,
922 L., Stepanek, C., Ueda, H., and Zhang, Z.: Challenges in quantifying Pliocene terrestrial warming
923 revealed by data-model discord, *Nature Clim. Change*, 3, 969-974, 10.1038/nclimate2008, 2013.

924 Schmidt, G. A., Ruedy, R., Hansen, J. E., Aleinov, I., Bell, N., Bauer, M., Bauer, S., Cairns, B.,
925 Canuto, V., Cheng, Y., Del Genio, A., Faluvegi, G., Friend, A. D., Hall, T. M., Hu, Y., Kelley, M.,
926 Kiang, N. Y., Koch, D., Lacis, A. A., Lerner, J., Lo, K. K., Miller, R. L., Nazarenko, L., Oinas, V.,
927 Perlwitz, J., Perlwitz, J., Rind, D., Romanou, A., Russell, G. L., Sato, M., Shindell, D. T., Stone, P.
928 H., Sun, S., Tausnev, N., Thresher, D., and Yao, M.-S.: Present-Day Atmospheric Simulations
929 Using GISS ModelE: Comparison to In Situ, Satellite, and Reanalysis Data, *Journal of Climate*,
930 19, 153-192, 10.1175/jcli3612.1, 2006.

931 Schuenemann, K. C., and Cassano, J. J.: Changes in synoptic weather patterns and Greenland
932 precipitation in the 20th and 21st centuries: 1. Evaluation of late 20th century simulations from IPCC
933 models, *Journal of Geophysical Research: Atmospheres*, 114, doi:10.1029/2009JD011705, 2009.

934 Seki, O., Foster, G. L., Schmidt, D. N., Mackensen, A., Kawamura, K., and Pancost, R. D.: Alkenone
935 and boron-based Pliocene pCO₂ records, *Earth and Planetary Science Letters*, 292, 201-211, 2010.

936 Sohl, L. E., Chandler, M. A., Schmunk, R. B., Mankoff, K., Jonas, J. A. , Foley, K. M., and Dowsett,
937 H. J.: PRISM3/GISS topographic reconstruction: U. S. , Geological Survey Data Series 419, 6p.,
938 2009.

939 Steffen, K., and Box, J.: Surface climatology of the Greenland ice sheet: Greenland Climate Network
940 1995-1999, *J. Geophys. Res.*, 106, 33951-33964, 10.1029/2001jd900161, 2001.

941 Stepanek, C., and Lohmann, G.: Modelling mid-Pliocene climate with COSMOS, *Geosci. Model Dev.*
942 *Discuss.*, 5, 917-966, 10.5194/gmdd-5-917-2012, 2012.

943 Stone, E. J., Lunt, D. J., Rutt, I. C., and Hanna, E.: Investigating the sensitivity of numerical model
944 simulations of the modern state of the Greenland ice-sheet and its future response to climate
945 change, *The Cryosphere*, 4, 397–417, doi:10.5194/tc-4-397-2010, 2010.

946 Stone, E. J., Lunt, D. J., Annan, J. D., and Hargreaves, J. C.: Quantification of the Greenland ice sheet
947 contribution to Last Interglacial sea level rise, *Clim. Past*, 9, 621-639, 10.5194/cp-9-621-2013,
948 2013.

949 Tarasov, L., and Peltier, W. R.: Greenland glacial history and local geodynamic consequences.
950 *Geophysical Journal International*, 150, 198-229, doi:10.1046/j.1365-246X.2002.01702.x, 2002.

951 Tarasov, L., and Peltier, W. R.: A geophysically constrained large ensemble analysis of the deglacial
952 history of the North American ice-sheet complex, *Quaternary Science Reviews*, 23, 359-388,
953 10.1016/j.quascirev.2003.08.004, 2004.

954 Thompson, R. S., and Fleming, R. F.: Middle Pliocene vegetation: reconstructions, paleoclimatic
955 inferences, and boundary conditions for climate modeling, *Marine Micropaleontology*, 27, 27-49,
956 10.1016/0377-8398(95)00051-8, 1996.

957 Thompson, S. L., and Pollard, D.: Greenland and Antarctic Mass Balances for Present and Doubled
958 Atmospheric CO₂ from the GENESIS Version-2 Global Climate Model, *Journal of Climate*, 10,
959 871-900, 1997.

960 van de Berg, W. J., van den Broeke, M., Ettema, J., van Meijgaard, E. and Kaspar, F.: Significant
961 contribution of insolation to Eemian melting of the Greenland ice sheet, *Nature Geosci*, 4, 679–
962 683, 2011.

963 Vaughan, D.G., Comiso J.C., Allison I., Carrasco J., Kaser G., Kwok R., Mote P., Murray T., Paul F.,
964 Ren J., Rignot E., Solomina O., Steffen K. and Zhang T.: Observations: Cryosphere. In: *Climate*
965 *Change 2013: The Physical Science Basis. Contribution of Working Group I to the Fifth*
966 *Assessment Report of the Intergovernmental Panel on Climate Change* [Stocker, T.F., D. Qin, G.-

967 K. Plattner, M. Tignor, S.K. Allen, J. Boschung, A. Nauels, Y. Xia, V. Bex and P.M. Midgley
968 (eds.]. Cambridge University Press, Cambridge, United Kingdom and New York, NY, USA.

969 Vizcaíno, M., Mikolajewicz, U., Jungclaus, J., and Schurgers, G.: Climate modification by future ice
970 sheet changes and consequences for ice sheet mass balance, *Climate Dynamics*, 34, 301-324, 2008.

971 Warren, S., and Wiscombe, W.: A model for the spectral albedo of snow II. Snow containing
972 atmospheric aerosols., *Journal of the Atmospheric Sciences*, 37, 2734-2745, 1980.

973 Wiscombe, W., and Warren, S.: A model for the spectral albedo of snow I, *Journal of the*
974 *Atmospheric Sciences*, 37, 2712-2733, 1980.

975 Yan, Q., Zhang, Z. S., Gao, Y., Wang, H. and Johannessen, O. M.: Sensitivity of the modeled present-
976 day Greenland Ice Sheet to climatic forcing and spin-up methods and its influence on future sea
977 level projections, *Journal of Geophysical Research: Earth Surface*, 118, 2174-2189,
978 doi:10.1002/jgrf.20156, 2013.

979 Yan, Q., Zhang, Z. S., Wang, H. J., Gao, Y. Q., and Zheng, W. P.: Set-up and preliminary results of
980 mid-Pliocene climate simulations with CAM3.1, *Geosci. Model Dev.*, 5, 289-297, 10.5194/gmd-5-
981 289-2012, 2012.

982 Yan, Q., Zhang, Z. S., Wang, H., and Zhang, R.: Simulation of Greenland ice sheet during the mid-
983 Pliocene warm period, *Chinese Science Bulletin*, 59, 201-211, 10.1007/s11434-013-0001-z, 2014.

984 Yukimoto, S., Noda, A., Kitoh, A., Hosaka, M., Yoshimora, H., Uchiyama, T., Shibata, K., Arakawa,
985 O., and Kusunoki, S.: Present-Day Climate and Climate Sensitivity in the Meteorological
986 Research Institute Coupled GCM Version 2.3 (MRI-CGCM2.3), *Journal of the Meteorological*
987 *Society of Japan*, 84, 333-363, 2006.

988 Zhang, R., Yan, Q., Zhang, Z. S., Jiang, D., Otto-Bliesner, B. L., Haywood, A. M., Hill, D. J., Dolan,
989 A. M., Stepanek, C., Lohmann, G., Contoux, C., Bragg, F., Chan, W. L., Chandler, M. A., Jost, A.,
990 Kamae, Y., Abe-Ouchi, A., Ramstein, G., Rosenbloom, N. A., Sohl, L., and Ueda, H.: Mid-
991 Pliocene East Asian monsoon climate simulated in the PlioMIP, *Clim. Past*, 9, 2085-2099,
992 10.5194/cp-9-2085-2013, 2013.

993 Zhang, Z. S., and Yan, Q.: Pre-industrial and mid-Pliocene simulations with NorESM-L: AGCM
994 simulations, *Geosci. Model Dev.*, 5, 1033-1043, 10.5194/gmd-5-1033-2012, 2012.

995 Zhang, Z. S., Nisancioglu, K., Bentsen, M., Tjiputra, J., Bethke, I., Yan, Q., Risebrobakken, B.,
996 Andersson, C., and Jansen, E.: Pre-industrial and mid-Pliocene simulations with NorESM-L,
997 *Geosci. Model Dev.*, 5, 523-533, 10.5194/gmd-5-523-2012, 2012.

998

999

1000

1001

1002

1003

1004

1005

1006

1007

1008

1009

1010

1011

1012

1013

1014

1015

1016 **Tables**

1017 **Table 1:** The short names of the PlioMIP climate models used to force BASISM, along with
 1018 the atmospheric component resolution and the land-sea mask (LSM) scheme implemented by
 1019 each model (Haywood et al., 2010). Regarding the LSM, ‘preferred’ refers to a LSM that has
 1020 been entirely altered to meet the PlioMIP boundary conditions, whereas ‘alternate’ is where
 1021 modelling groups have had to use more similar to modern LSM. More comprehensive details
 1022 of each model, and their implementation of the LSM, can be found in Haywood et al (2013)
 1023 and the individual references listed in this table.

1024

| Type | Model Name | Atmosphere Resolution (lat/lon) | References/Contributors | Preferred or Alternate LSM |
|----------|----------------------|---------------------------------|-----------------------------|----------------------------|
| AGCMs | CAM3.1 | ~2.8° × 2.8° (T42) | Yan et al. (2012) | Alternate |
| | COSMOS | 3.75° × 3.75° | Stepanek and Lohmann (2012) | Preferred |
| | HadAM3 | 2.5° × 3.75° | Bragg et al. (2012) | Preferred |
| | LMDZ5A | 1.9° × 3.75° | Contoux et al. (2012) | Preferred |
| | MIROC4m | ~2.8° × 2.8° (T42) | Chan et al. (2011) | Preferred |
| | MRI-CGCM2.3 | ~2.8° × 2.8° (T42) | Kamae and Ueda (2012) | Alternate |
| | NorESM-L | ~3.75° × 3.75° (T31) | Zhang and Yan (2012) | Alternate |
| AOGCMs | CCSM4 | 0.9° × 1.25° | Rosenbloom et al. (2013) | Alternate |
| | COSMOS | 3.75° × 3.75° | Stepanek and Lohmann (2012) | Preferred |
| | GISS ModelE2-R | 2° × 2.5° | Chandler et al. (2013) | Preferred |
| | HadCM3 | 2.5° × 3.75° | Bragg et al. (2012) | Alternate |
| | IPSLCM5A | 1.9° × 3.75° | Contoux et al. (2012) | Alternate |
| | MIROC4m | ~2.8° × 2.8° (T42) | Chan et al. (2011) | Preferred |
| | MRI-CGCM2.3 | ~2.8° × 2.8° (T42) | Kamae and Ueda (2012) | Alternate |
| NorESM-L | ~3.75° × 3.75° (T31) | Zhang et al. (2012) | Alternate | |

1025

1026

1027 **Table 2:** The three glaciological parameters and the values considered in the ice sheet
1028 modelling simulations. By varying each glaciological parameter independently, while
1029 holding the others constant, there are a total of 48 sensitivity experiments performed for each
1030 ice sheet model simulation.

1031

| Lapse Rate ($^{\circ}\text{C km}^{-1}$) | PDD Factor Snow (α_i ; $\text{mm day}^{-1} \text{ }^{\circ}\text{C}^{-1}$) | PDD Factor Ice (α_s ; $\text{mm day}^{-1} \text{ }^{\circ}\text{C}^{-1}$) |
|--|--|---|
| -6 | 3 | 5 |
| -7 | 4 | 6 |
| -8 | 5 | 8 |
| | 6 | 14 |

1032

1033

1034 **Table 3:** Mean annual and summer temperature and mean annual precipitation values over
 1035 the Greenland region for the PlioMIP climate models for the pre-industrial control
 1036 experiments and the mPWP simulations. The climatological values have been calculated
 1037 over the entire Greenland land mass as defined by the individual land-sea masks prescribed in
 1038 the climate models. No ocean temperatures/precipitation values have been used.
 1039

| | | Greenland | | | |
|-----------------|-----------------------|-------------------|----------------|--|------|
| | Abbrev. Model Name | Temperature (°C) | | Precipitation | |
| | | Mean Annual | Mean Summer | Mean Annual (mm day ⁻¹) | |
| AGCMs | Pre-Industrial | CAM3.1 | -14.36 | -1.76 | 1.56 |
| | | COSMOS | -18.22 | -5.48 | 1.21 |
| | | HadAM3 | -22.59 | -8.82 | 0.92 |
| | | LMDZ5A | -20.97 | -6.16 | 0.81 |
| | | MIROC4m | -19.44 | -2.09 | 0.92 |
| | | MRI- CGCM2.3 | -20.50 | -12.23 | 1.04 |
| | | NorESM-L | -13.97 | -1.71 | 1.33 |
| | mid-Pliocene | CAM3.1 | -2.45 | 8.95 | 2.01 |
| | | COSMOS | -4.26 | 7.41 | 2.00 |
| | | HadAM3 | -8.98 | 4.09 | 1.70 |
| | | LMDZ5A | -6.89 | 7.69 | 1.92 |
| | | MIROC4m | -6.24 | 7.33 | 1.67 |
| | | MRI- CGCM2.3 | -7.37 | 1.53 | 1.65 |
| | | NorESM-L | -0.71 | 13.00 | 1.70 |
| AOGCMs | Pre-Industrial | CCSM4 | -20.74 | -5.08 | 1.25 |
| | | COSMOS | -18.32 | -4.74 | 1.20 |
| | | GISS ModelE2-R | -14.78 | -5.69 | 0.64 |
| | | HadCM3 | -22.21 | -10.14 | 1.05 |
| | | IPSLCM5A | -24.68 | -7.76 | 0.56 |
| | | MIROC4m | -19.65 | -2.46 | 0.94 |
| | | MRI- CGCM2.3 | -28.18 | -19.60 | 0.70 |
| | mid-Pliocene | NorESM-L | -15.86 | -2.73 | 1.26 |
| | | CCSM4 | -13.58 | 5.42 | 1.60 |
| | | COSMOS | -5.93 | 8.08 | 1.83 |
| | | GISS ModelE2-R | -9.44 | 9.32 | 0.85 |
| | | HadCM3 | -10.09 | 4.24 | 1.69 |
| | | IPSLCM5A | -11.89 | 7.12 | 1.34 |
| | | MIROC4m | -7.36 | 9.15 | 1.52 |
| MRI- CGCM2.3 | -19.18 | -15.59 | 0.96 | | |
| NorESM-L | -3.60 | 12.04 | 1.55 | | |

1040

1041 **Table 4:** GrIS diagnostics for the PlioMIP simulations, including volume, sea level
 1042 equivalent and ice area using the standard BASISM parameters. Values are given as a
 1043 difference from the simulated pre-industrial GrIS, when the same GCM pre-industrial forcing
 1044 climatology is used. For example, negative volume or area means that the GrIS reduces in
 1045 size compared to the GCM pre-industrial control. All simulated volumes (foe each parameter
 1046 set) can be found in the Supplementary Information (Table S1).

1047

| | Model Name | Volume ($\times 10^6$ km ³) | S.L.E. (m) | Area ($\times 10^6$ km ²) |
|--------|-----------------|---|---------------|---|
| AGCMs | CAM3.1 | -2.70 | -6.89 | -1.10 |
| | COSMOS | 0.14 | 0.36 | -0.07 |
| | HadAM3 | -1.27 | -3.25 | -0.63 |
| | LMDZ5A | -1.67 | -4.25 | -0.85 |
| | MIROC4m | 0.19 | 0.49 | -0.04 |
| | MRI- CGCM2.3 | 0.22 | 0.57 | -0.01 |
| | NorESM-L | -3.46 | -8.82 | -1.66 |
| | ----- | | | |
| AOGCMs | CCSM4 | -0.27 | -0.68 | -0.24 |
| | COSMOS | -0.66 | -1.68 | -0.36 |
| | GISS | -1.89 | -4.82 | -0.96 |
| | ModelE2-R | | | |
| | HadCM3 | -1.73 | -4.42 | -0.83 |
| | IPSLCM5A | -1.85 | -4.71 | -0.91 |
| | MIROC4m | -0.83 | -2.13 | -0.44 |
| | MRI- CGCM2.3 | 0.20 | 0.50 | 0.00 |
| | NorESM-L | -3.12 | -7.94 | -1.41 |

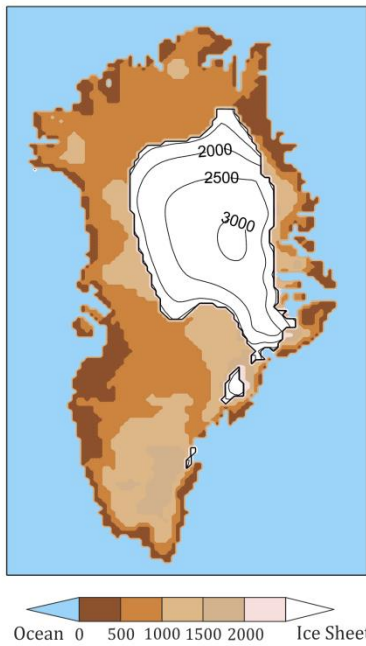
1048

1049

1050

| Model | Snow albedo dependent on Temperature? | Aging snow simulated? | Wet/dry snow albedo properties considered? | Dependent upon the solar zenith angle? | Radiative effects of darkening snow considered? | General References |
|---------------------|---|--|---|--|--|--|
| CAM3.1 | Yes - albedo dependent on temperature and spectral band to distinguish albedos for direct and diffuse incident radiation. | No | Yes – through temperature dependence | No – Ebert and Curry (1993) | <i>Unknown</i> | Collins et al. (2004) |
| CCSM4 | Yes, snow albedo is an indirect function of temperature through the impact of temperature on snow grain size in the SNICAR model (SNOW, ICe, and Aerosol Radiative model; Flanner and Zender, 2006) | Yes - through the SNICAR model | Yes - through the effective ice grain size which is altered by liquid water-induced metamorphism and refreezing | Yes | Yes - snow darkening occurs due to snow aging as well as black carbon and dust deposition (SNICAR) | Gent et al. (2011); Lawrence et al. (2011) |
| COSMOS | Yes – assumed to be a linear function of surface temperature. minimum $\alpha = 0.6$ for melting snow and maximum $\alpha = 0.8$ for cold temperatures | No | Yes - through temperature dependence | No | Yes – through temperature dependence | Roeckner et al. (2003) |
| GISS ModelE2-R | <i>Unknown</i> | Yes – following Loth and Graf (1998) | Yes - following Wiscombe and Warren (1980) | Yes – following Wiscombe and Warren (1980) | Yes – following Warren and Wiscombe (1980) | Schmidt et al. (2006) |
| HadAM3/ HadCM3 | Yes – Uses land surface energy scheme MOSES1 (Cox et al., 1999) and albedo of snow is temperature dependent | No | No | <i>Unknown</i> | No | Cox et al. (1999) |
| LMDZ5A/ IPSLCM5A | No – snow albedo is dependent on snow age (as a function of time since the last snowfall). Land surface model is ORCHIDEE (Organizing Carbon and Hydrology In Dynamic Ecosystems, Krinner et al., 2005) | Yes | No | No | Yes – through the snow aging process | (Krinner et al., 2005) |
| MIROC4m | <i>Unknown</i> | Yes - following Wiscombe and Warren (1980) | Yes - following Wiscombe and Warren (1980) | Yes - following Wiscombe and Warren (1980) | Yes - following Wiscombe and Warren (1980) | Numaguti et al. (1997) |
| MRI-CGCM2.3 | Yes – snow albedo ranges from from 0.8 (at temperatures $< -4^{\circ}\text{C}$) to 0.64 (where the temperature of snow is 0°C ; melting snow) | No | Yes - through temperature dependence | No | No | Yukimoto et al. (2006) |
| NorESM-L | As in CCSM4 | As in CCSM4 | As in CCSM4 | As in CCSM4 | As in CCSM4 | As in CCSM4 |

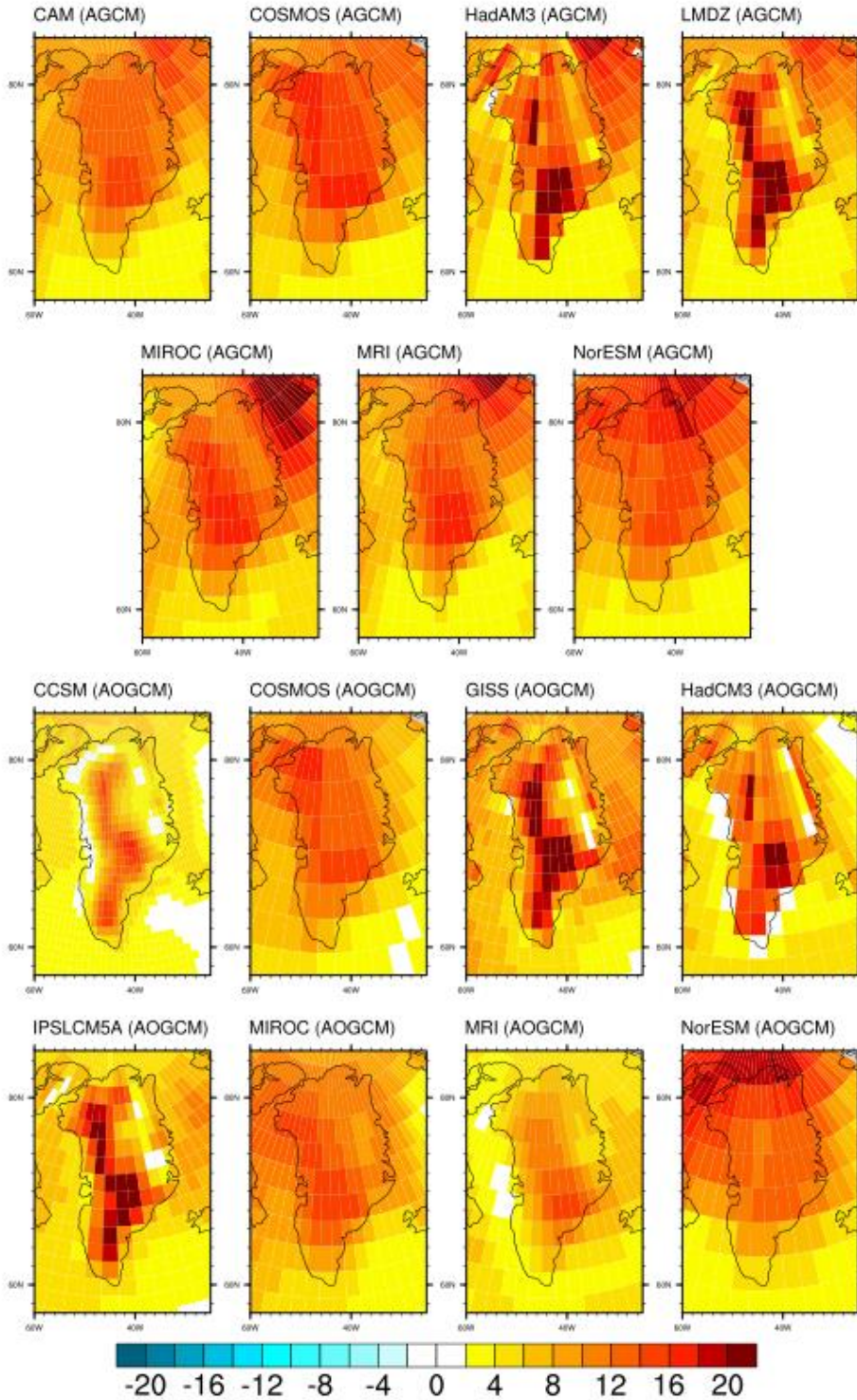
Table 5: Details of snow albedo properties over land in each of the PlioMIP climate models.



1054

1055 **Figure 1:** The PRISM3 Greenland ice sheet as simulated by BASISM (Hill, 2009; Dowsett et
1056 al., 2010). The forcing climatology for this ice sheet reconstruction is a HadAM3 simulation
1057 with PRISM2 boundary conditions (as described in Salzmann et al., 2008).

1058



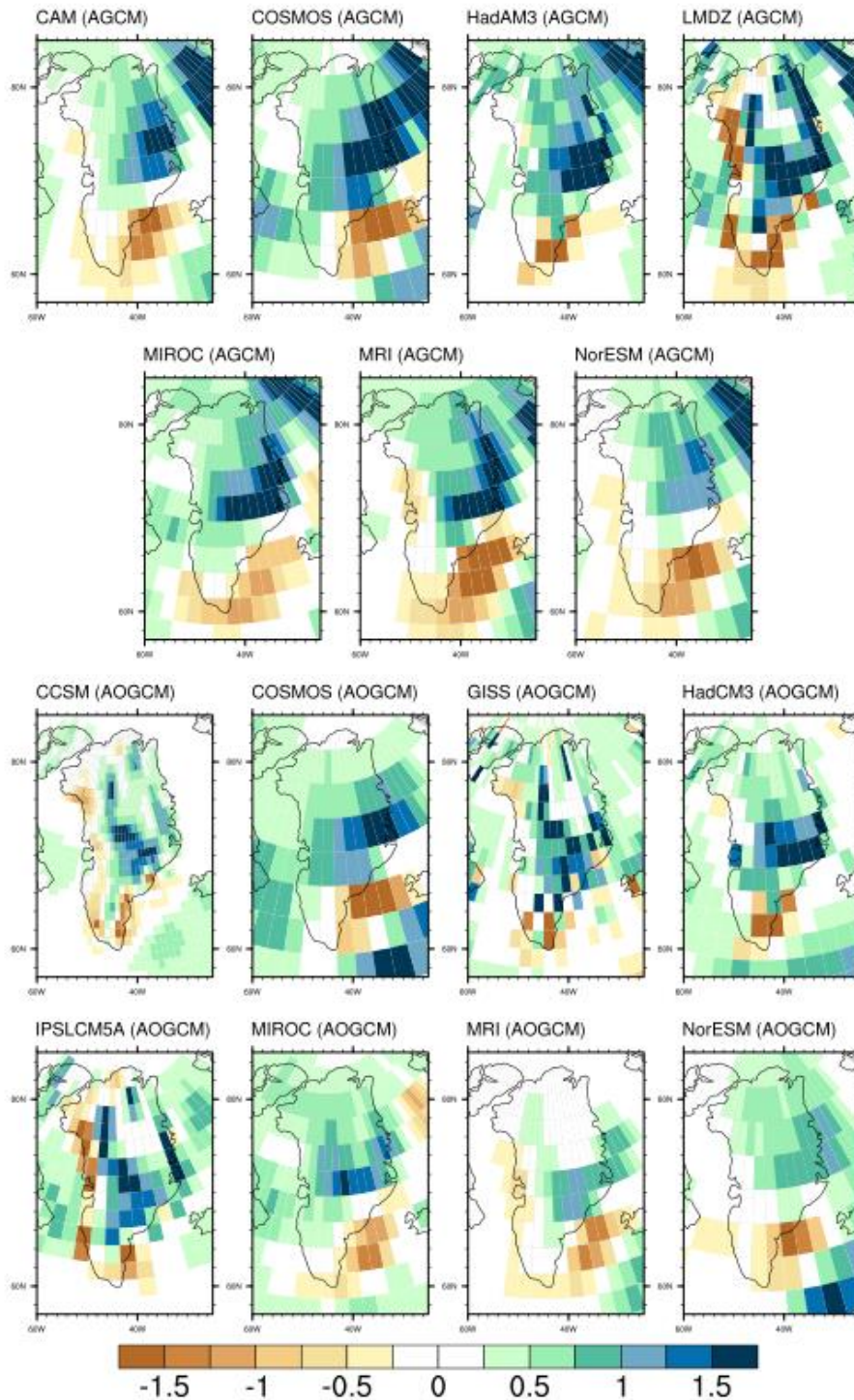
1059

1060

Figure 2: Pliocene minus pre-industrial mean annual surface air temperature (°C) over Greenland for the PlioMIP ensemble using atmosphere-only (AGCMs) and coupled atmosphere-ocean climate models (AOGCMs). Temperature plotted on the original climate model resolution.

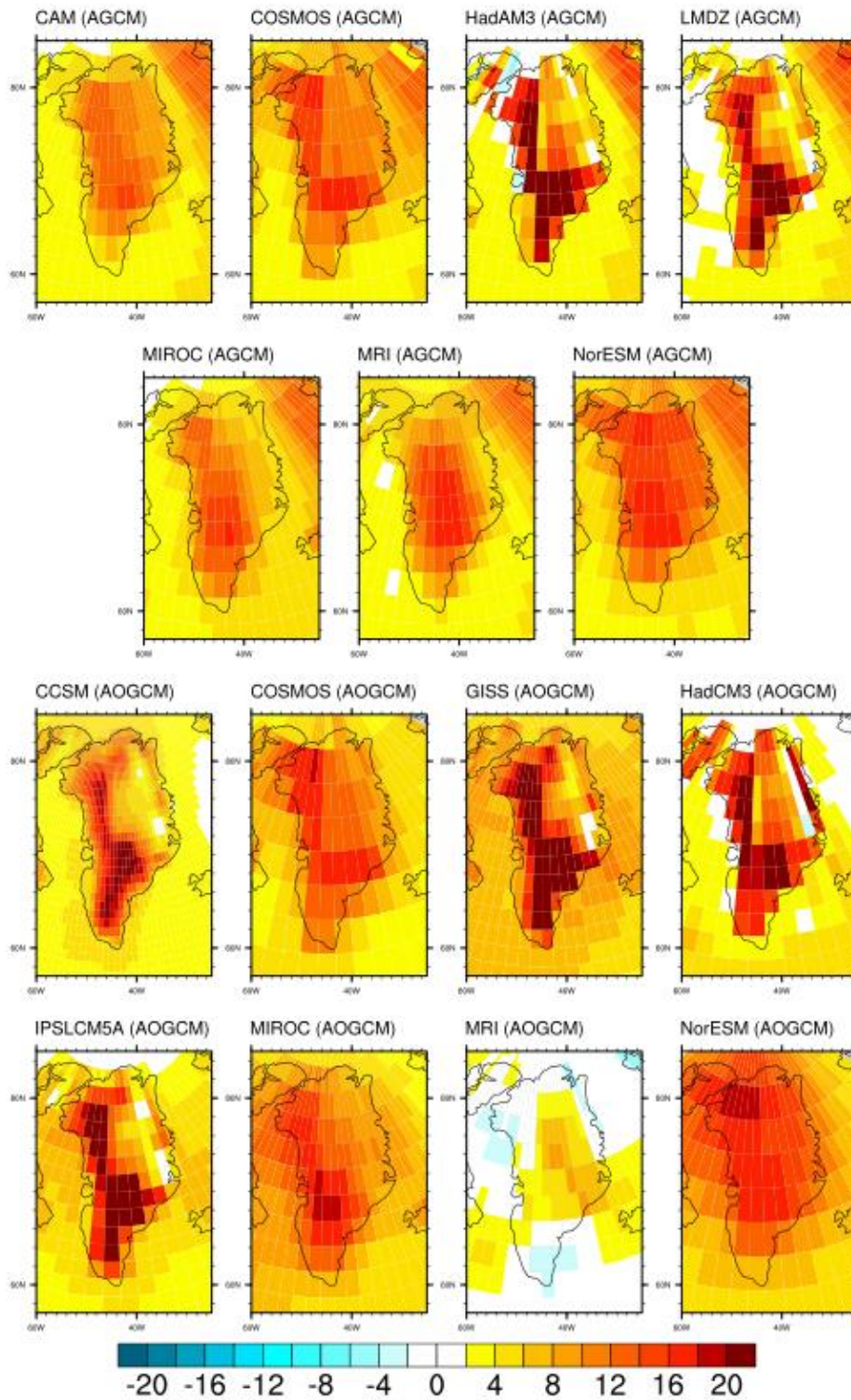
1062

1063



1064

1065 **Figure 3:** Pliocene minus pre-industrial mean annual precipitation (mm day^{-1}) over Greenland for the
 1066 PliomIP ensemble using atmosphere-only (AGCMs) and coupled atmosphere-ocean climate models
 1067 (AOGCMs). Precipitation plotted on the original climate model resolution.



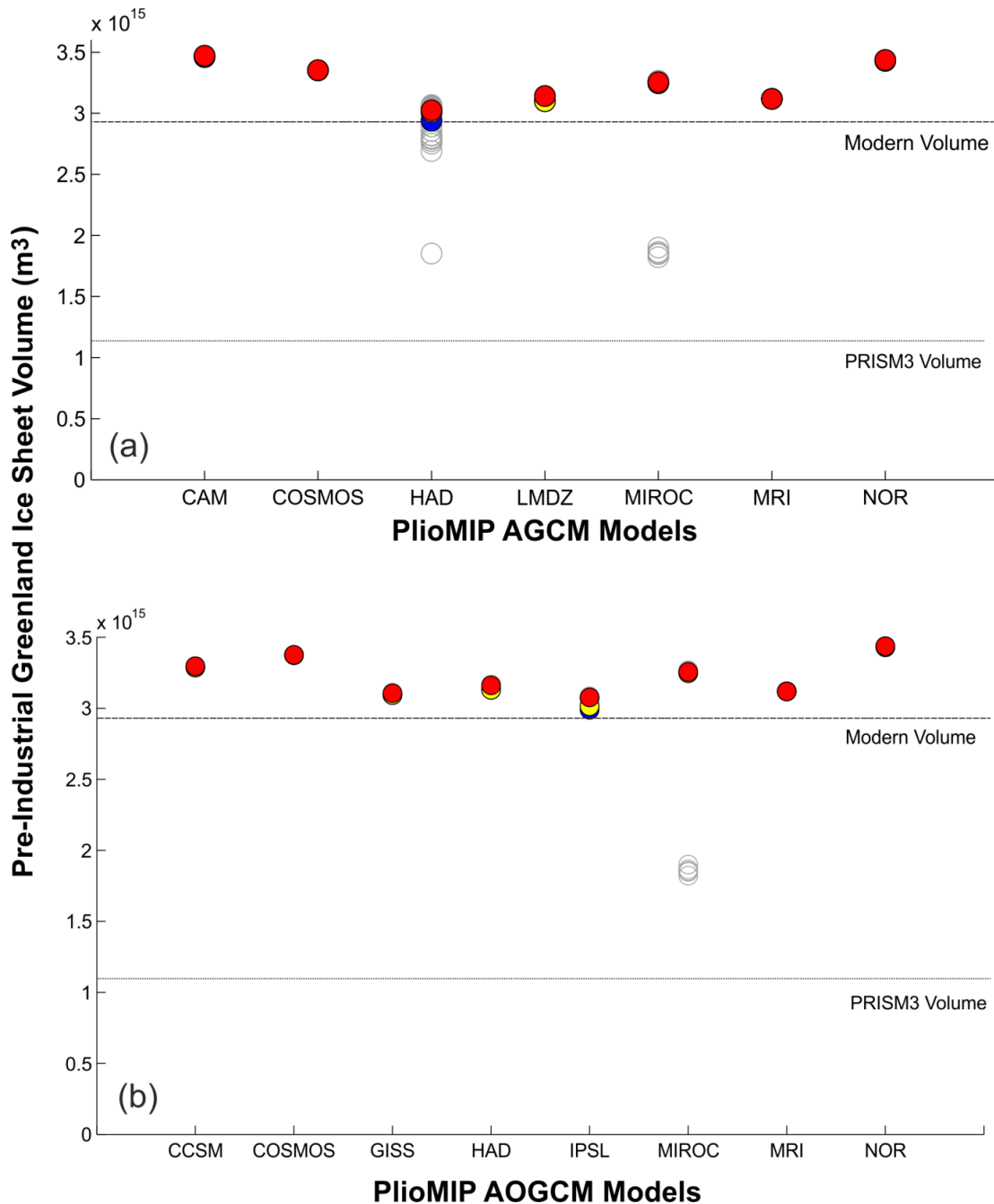
1068

1069

1070

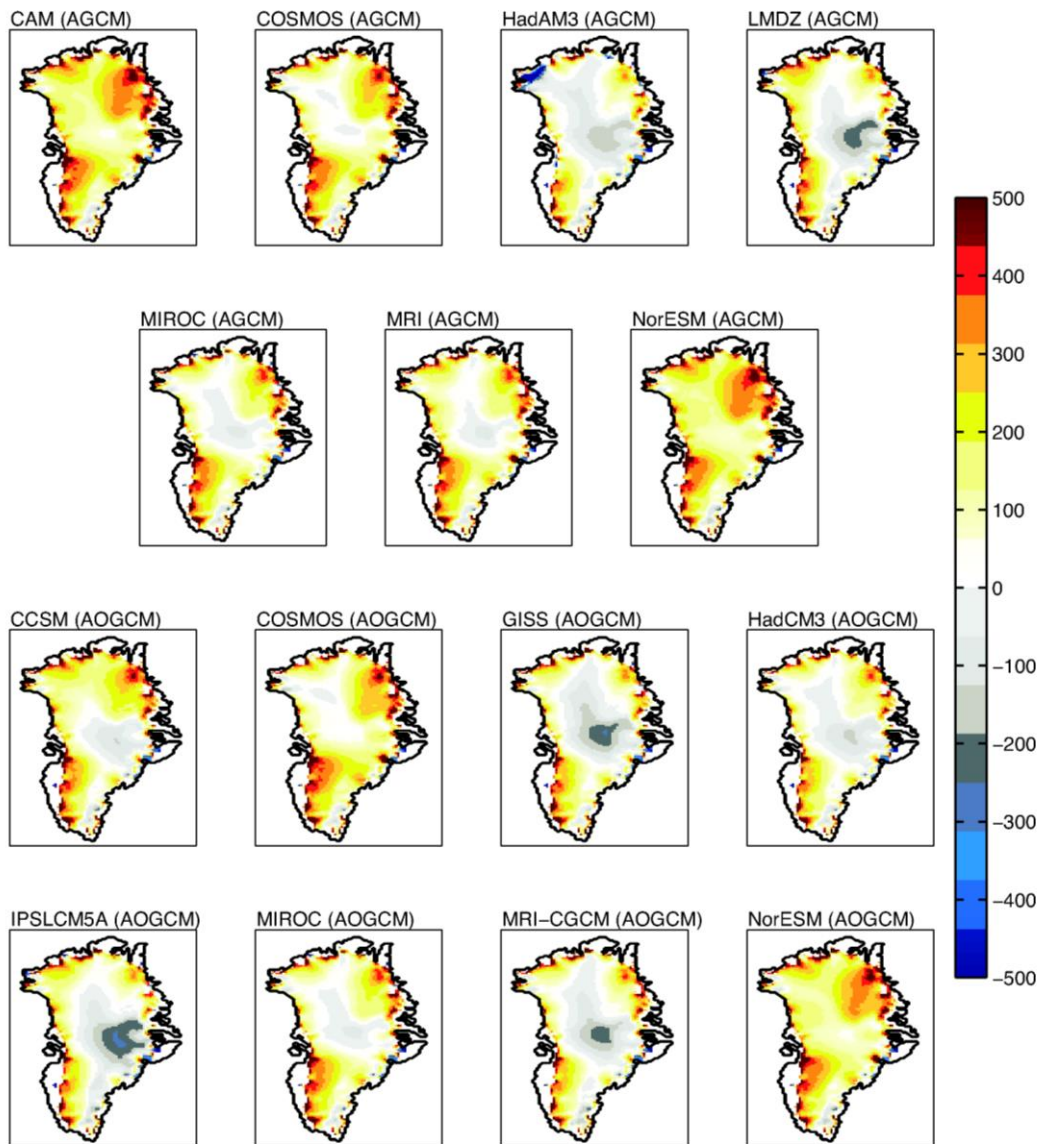
1071

Figure 4: Pliocene minus pre-industrial mean July surface air temperature (°C) over Greenland for the PlioMIP ensemble using atmosphere-only (AGCMs) and coupled atmosphere-ocean climate models (AOGCMs). Temperature plotted on the original climate model resolution.



1072

1073 **Figure 5:** Simulated GrIS volume when BASISM is forced with the pre-industrial climatology from
 1074 each of the (a) AGCM and (b) AOGCM PlioMIP models. The volume of the observed present-day
 1075 GrIS (Bamber et al., 2001a) is shown for comparison. Red-filled circles show the standard parameter
 1076 set used within BASISM ($\alpha_i = 8 \text{ mm day}^{-1} \text{ }^\circ\text{C}^{-1}$ and $\alpha_s = 3 \text{ mm day}^{-1} \text{ }^\circ\text{C}^{-1}$, lapse rate = -6°C km^{-1}) and
 1077 blue-filled circles show the parameter set that gives a volumetric reconstruction closest to observed.
 1078 Yellow-filled circles show the parameter set that gives the lowest RMSE in terms of thickness. Grey
 1079 circles show the sensitivity of the ice sheet volume to different values of lapse rate and the PDD
 1080 factors for ice and snow (see Table 2). The coloured circles are superimposed on the grey circles, so
 1081 when the GrIS volume is similar, the grey circles (or individual colours) will not be visible.



1083

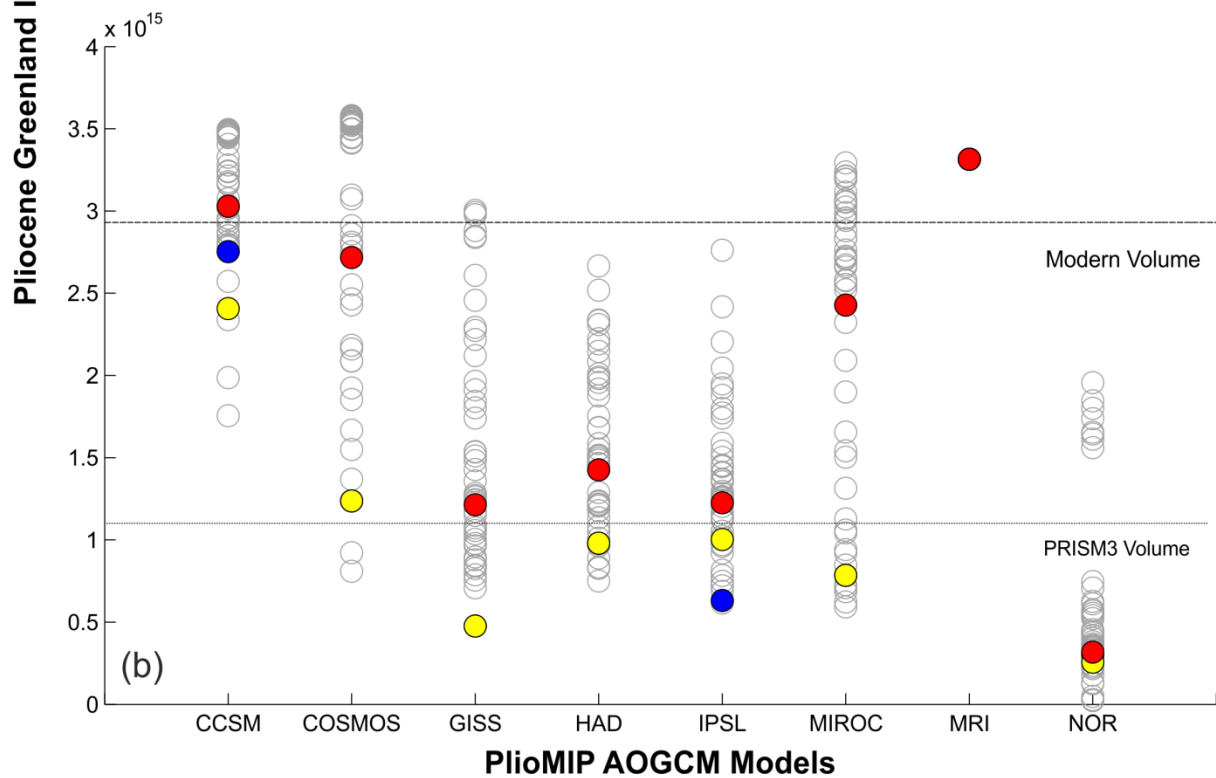
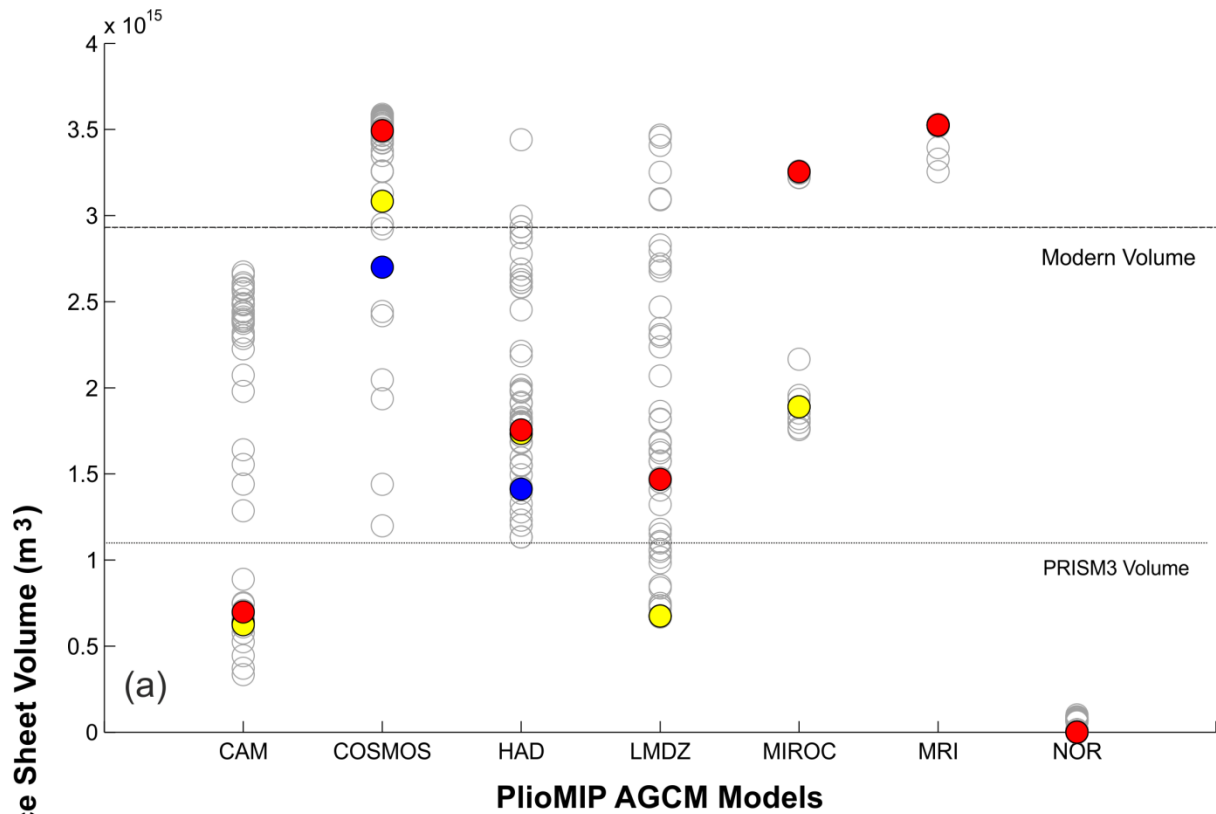
1084 **Figure 6:** Ice sheet surface elevation (m) anomalies (model minus data) for the pre-industrial control
 1085 relative to the observed present-day GrIS (Bamber et al., 2001) for individual AGCM and AOGCM
 1086 forcings. The BASISM simulations shown here were run using BASISM's standard glaciological
 1087 parameters ($\alpha_s = 3 \text{ mm day}^{-1} \text{ }^\circ\text{C}^{-1}$ and $\alpha_i = 8 \text{ mm day}^{-1} \text{ }^\circ\text{C}^{-1}$, lapse rate = -6°C km^{-1}).

1088

1089

1090

1091

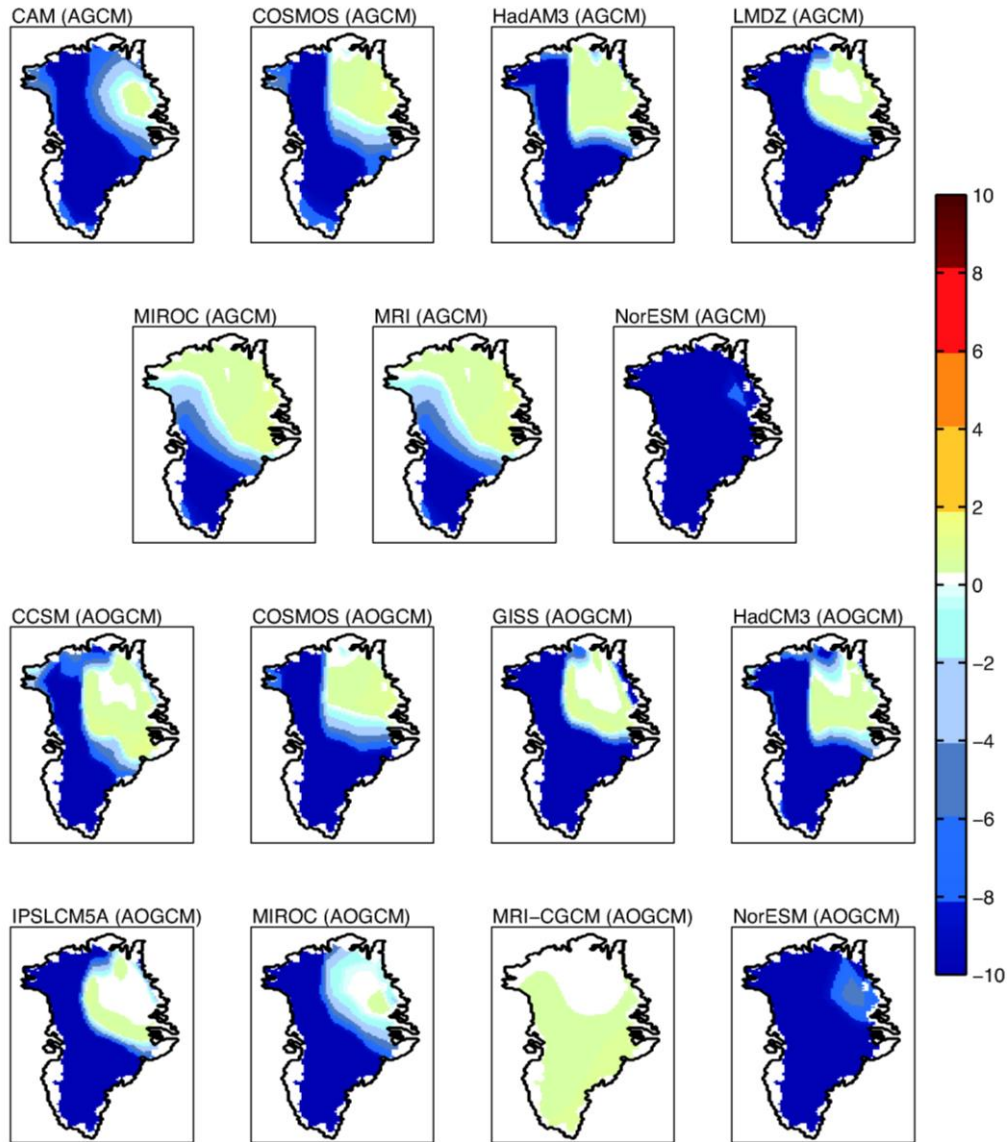


1092
1093
1094
1095
1096
1097

Figure 7: Simulated GrIS volume when BASISM is forced with the Pliocene climatology from each of the (a) AGCM and (b) AOGCM PlioMIP models. The volume of the observed present-day GrIS (Bamber et al., 2001a) is shown for comparison. Red-filled circles show the standard parameter set used within BASISM ($\alpha_i = 8 \text{ mm day}^{-1} \text{ }^\circ\text{C}^{-1}$ and $\alpha_s = 3 \text{ mm day}^{-1} \text{ }^\circ\text{C}^{-1}$, lapse rate = -6°C km^{-1}) and blue-filled circles show the parameter set that gives a volumetric reconstruction closest to observed.

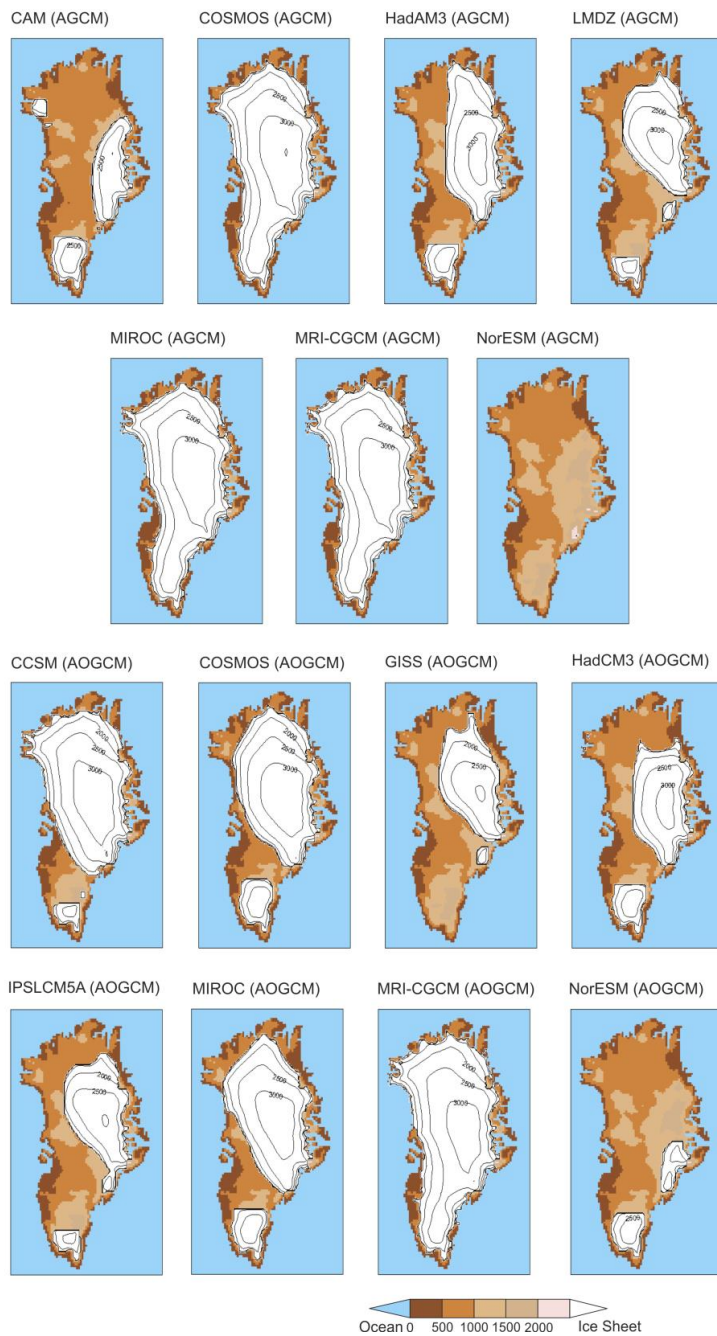
1098 Yellow-filled circles show the parameter set that gives the smallest RMSE in terms of simulated ice
 1099 sheet thickness. Grey circles show the sensitivity of the ice sheet volume to different values of lapse
 1100 rate and the PDD factors for ice and snow (see Table 2). The coloured circles are superimposed on
 1101 the grey circles, so when the GrIS volume is similar, the grey circles (or individual colours) will not
 1102 be visible.

1103



1104

1105 **Figure 8:** BASISM Surface Mass Balance (SMB; m yr^{-1}) predictions for the Pliocene (on the ISM
 1106 grid) derived from the PliomIP climatologies and using standard glaciological parameters ($\alpha_i = 8 \text{ mm}$
 1107 $\text{day}^{-1} \text{ }^\circ\text{C}^{-1}$ and $\alpha_s = 3 \text{ mm day}^{-1} \text{ }^\circ\text{C}^{-1}$, lapse rate = -6°C km^{-1}). The SMB is plotted for the first time
 1108 step (prior to a lapse rate correction) and shows areas of ablation (negative SMB) and accumulation
 1109 (positive SMB) based on the temperature and precipitation fields shown in Figures 2, 3 and 4.

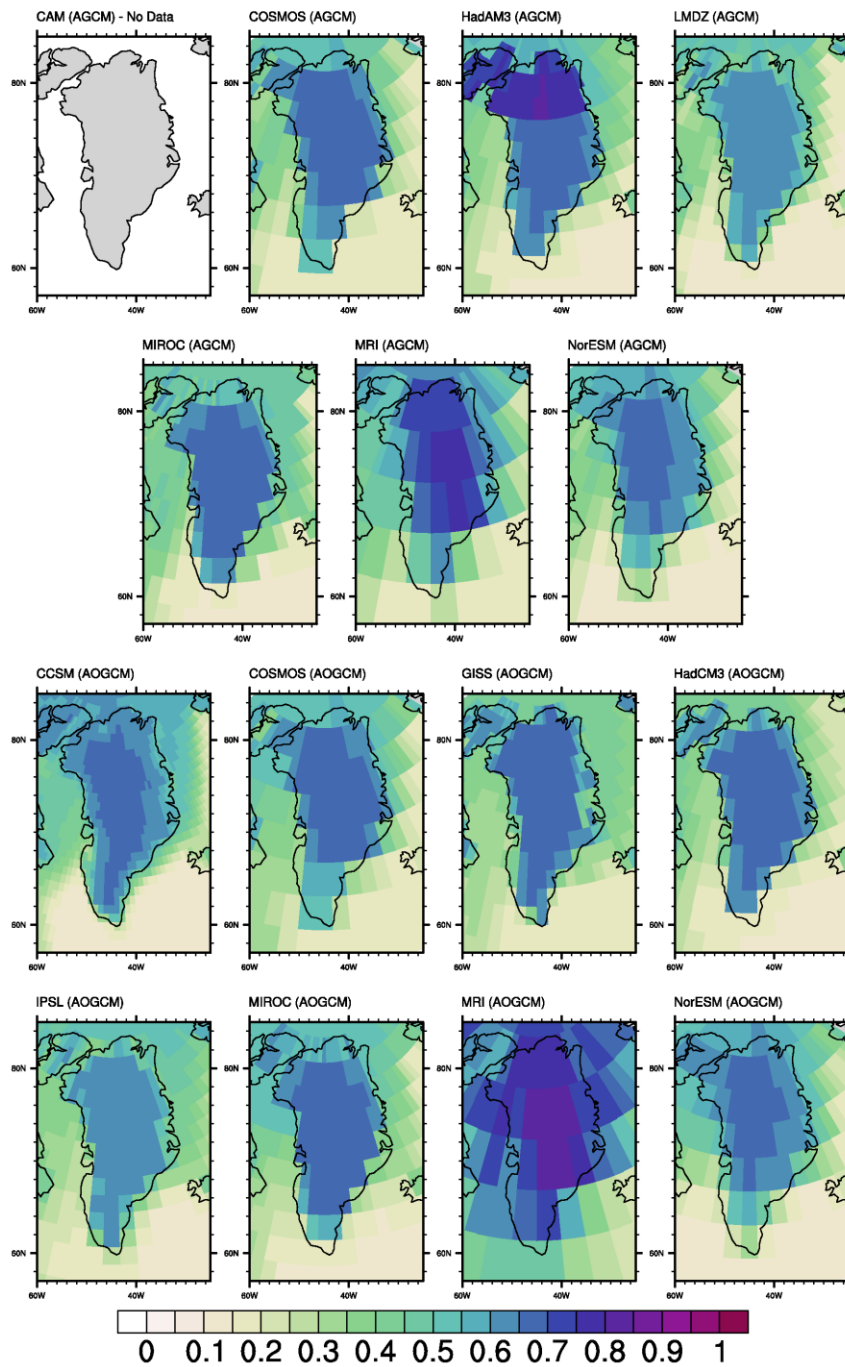


1110

1111 **Figure 9:** BASISM reconstructions of the Pliocene GrIS for individual AGCM and AOGCM
 1112 forcings. All BASISM simulations were forced with climate model fields (i.e. temperature and
 1113 precipitation) that were downscaled by a bilinear interpolation method from the original model grid to
 1114 $20 \text{ km} \times 20 \text{ km}$ resolution. GCM specific topography was also used and the ISM simulations were
 1115 initialised from the PRISM3 ice sheet configuration (Fig. 1). The ice sheet configurations relate to the
 1116 volumes (red-filled circles) shown in Figure 7 which use standard glaciological parameters.

1117

Pre-Industrial Albedo Values over Greenland (α)

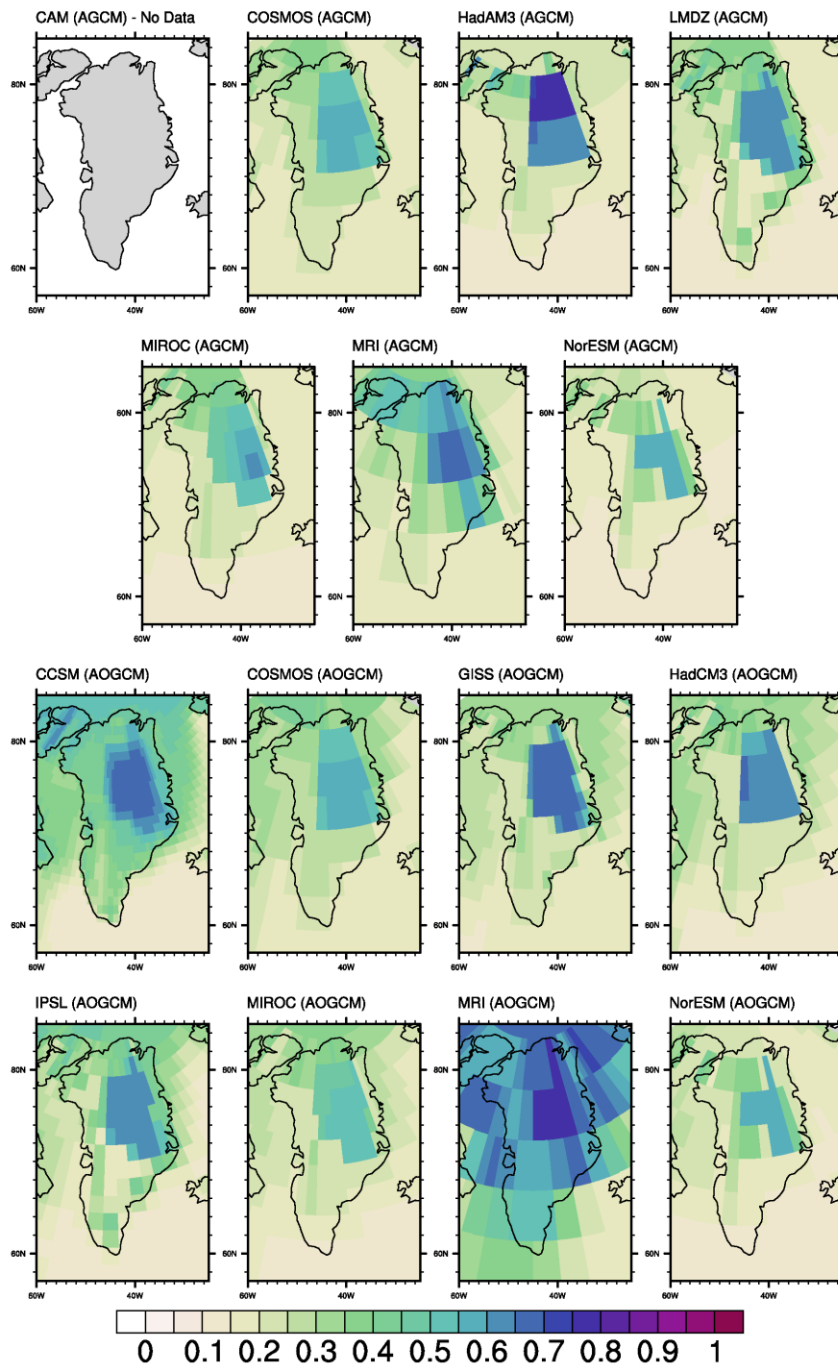


1118

1119 **Figure 10:** Pre-industrial annual mean clear sky albedo values over Greenland for PlioMIP models

1120 (where available).

Pliocene Albedo Values over Greenland (α)



1121

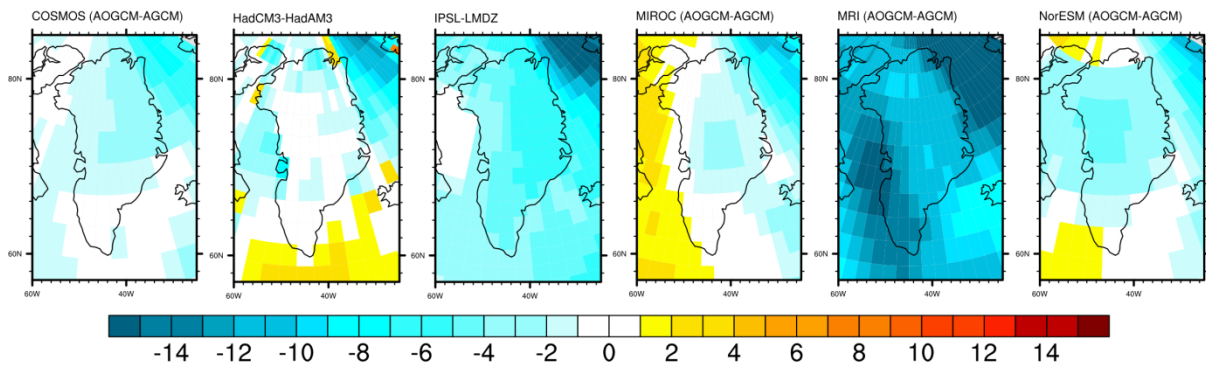
1122 **Figure 11:** Mid-Pliocene annual mean clear sky albedo values over Greenland for PlioMIP models
1123 (where available).

1124

1125

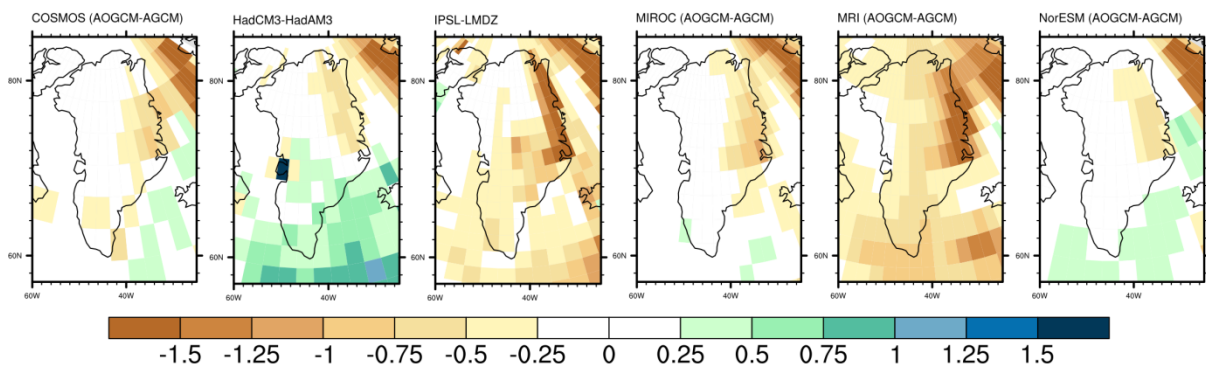
Mean Annual Temperature Comparison

(°C)



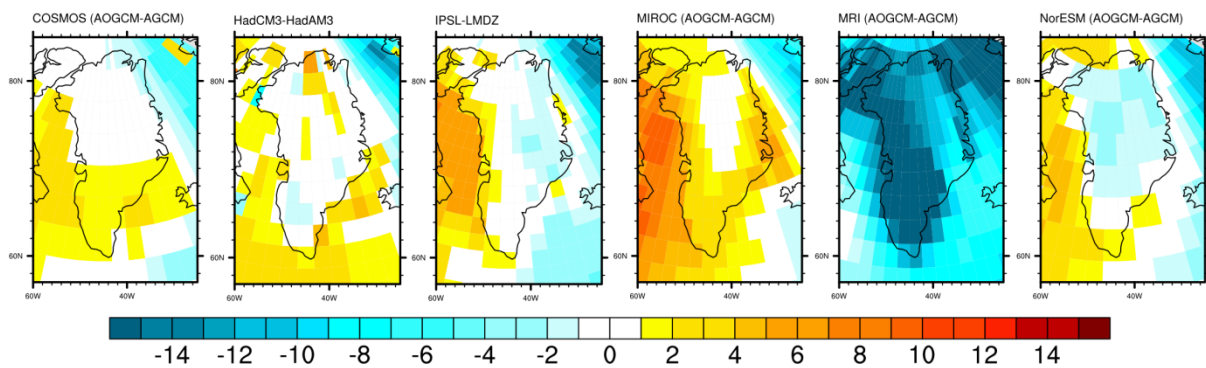
Mean Annual Precipitation Comparison

(mm day⁻¹)



Mean July Temperature Comparison

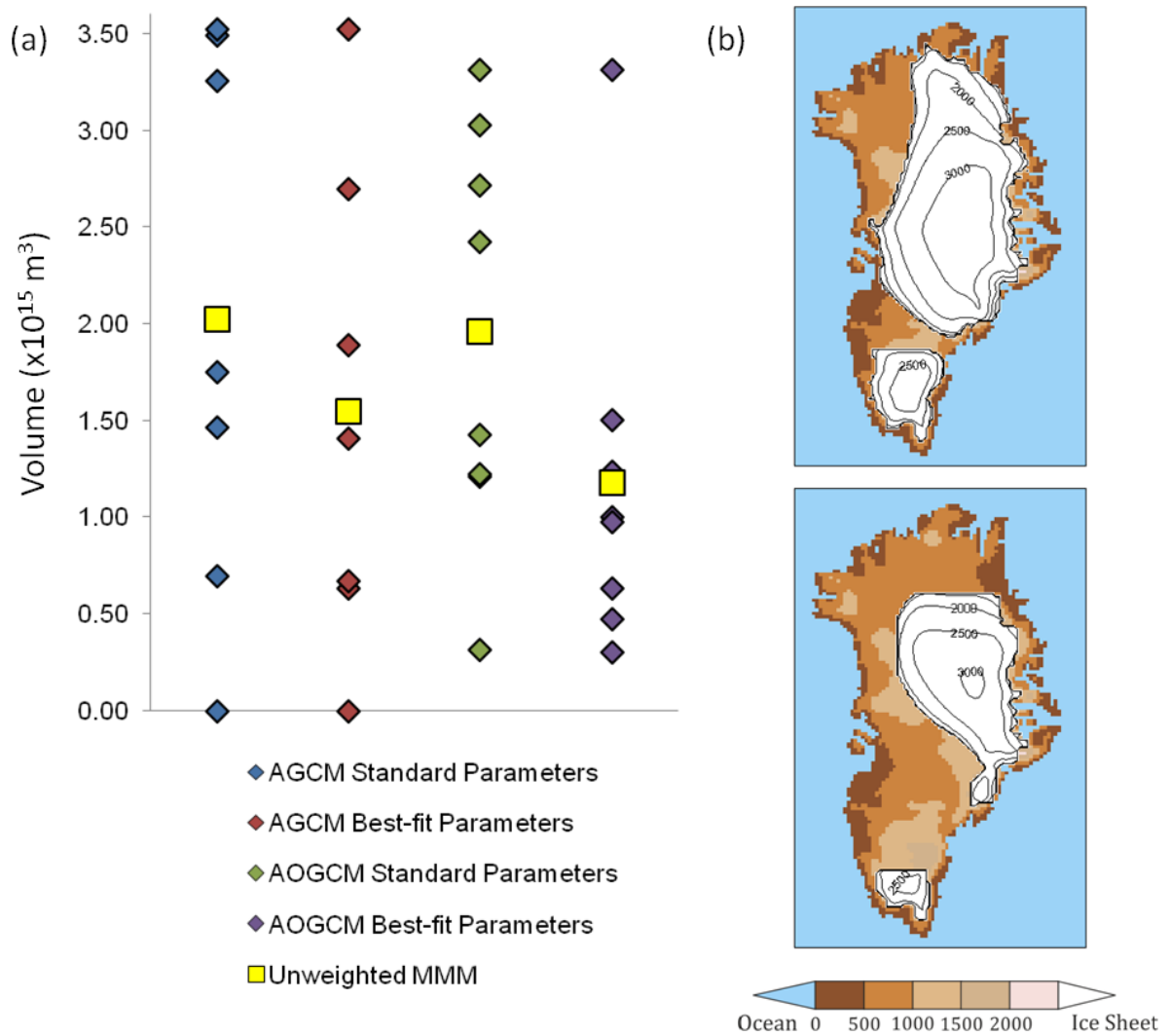
(°C)



1126
1127

1128 **Figure 12:** Pliocene mean annual temperature (°C) and precipitation (mm day⁻¹), and mean July
1129 temperature differences simulated between the AOGCMs and AGCMs over Greenland for
1130 comparable models from the PlioMIP ensemble (AOGCM climate minus AGCM climate).

1131



1132

1133 **Figure 13:** (a) Summary of the spread of mid-Pliocene GrIS volumes for each model within the
 1134 PliomIP ensemble (AGCM and AOGCM) compared with the un-weighted MMM for either the
 1135 standard BASISM glaciological parameter set or for the parameter set that gives the ‘best’ volumetric
 1136 representation of the modern GrIS. (b) Ice sheet configuration with the closest volume equating to
 1137 the largest (top) and smallest (bottom) MMM volume.

1138

1139

1140

1141

1142

1143

1144 **Supplementary Information: Using results from the PlioMIP ensemble to investigate the**
 1145 **Greenland Ice Sheet during the mid-Pliocene warm period**

1146 Supplementary Table 1: GrIS diagnostics for the PlioMIP simulations, including volume and ice area using the
 1147 different parameter sets described as shown by the coloured circles in Figures 5 and 7. Values are given as a
 1148 difference from the simulated pre-industrial GrIS, when the same GCM pre-industrial forcing climatology is
 1149 used. For example, negative volume or area means that the GrIS reduces in size compared to the GCM pre-
 1150 industrial control.

1151

| | Model Name | Standard parameter set used within BASISM (Red circles) | Parameter set | |
|---------------|-------------------|---|--|--|
| | | | that gives a volumetric reconstruction closest to observed (Blue circles) | Parameter set that gives the lowest RMSE in terms of thickness (Yellow circles) |
| | | Volume ($\times 10^6 \text{ km}^3$) | Volume ($\times 10^6 \text{ km}^3$) | Volume ($\times 10^6 \text{ km}^3$) |
| AGCMs | CAM3.1 | -2.70 | -2.83 | -2.84 |
| | COSMOS | 0.14 | -0.65 | -0.27 |
| | HadAM3 | -1.27 | -1.53 | -1.28 |
| | LMDZ5A | -1.67 | -2.42 | -2.42 |
| | MIROC4m | 0.19 | -1.36 | -1.36 |
| | MRI- CGCM2.3 | 0.22 | 0.41 | 0.41 |
| | NorESM-L | -3.46 | -3.43 | -3.43 |
| AOGCMs | CCSM4 | -0.27 | -0.53 | -0.88 |
| | COSMOS | -0.66 | -2.14 | -2.14 |
| | GISS ModelE2-R | -1.89 | -2.62 | -2.62 |
| | HadCM3 | -1.73 | -2.15 | -2.15 |
| | IPSLCM5A | -1.85 | -2.36 | -2.01 |
| | MIROC4m | -0.83 | -2.46 | -2.46 |
| | MRI- CGCM2.3 | 0.20 | 0.20 | 0.20 |
| | NorESM-L | -3.12 | -3.13 | -3.18 |

1152